2005 August
Master's Thesis

A Study on the Stern Design of a 200,000m^3 LNG Carrier

Graduate School of Chosun University

Department of Naval Architecture and Ocean Engineering

Karl Isaacs

A Study on the Stern Design of a 200,000m^3 LNG Carrier

200,000m^{3}급 LNG선의 선미설계에 관한 연구

August 2005

Graduate School of Chosun University

Department of Naval Architecture and Ocean Engineering

Karl Isaacs

A Study on the Stern Design of a 200,000m^3 LNG Carrier

Advisor: Professor Kwi-Joo Lee

Thesis submitted for the degree of Master of Engineering

August 2005

Graduate School of Chosun University

Department of Naval Architecture and
Ocean Engineering

Karl Isaacs

Master Thesis approved by

Dr. Igor Shugan
Chosun University _____

Prof. Lee, Kwi Joo
Chosun University _____

Prof. Yoon, Duck Young
Chosun University _____

May 2005

Chosun University Graduate School

- Contents -

List of Figures

List of Tables

ABSTRACT

A Study on the Stern Design of a 200,000m^3 LNG Carrier

Karl Isaacs
Advisor: Prof. Lee, Kwi- Joo
Chosun University Graduate School
Department of Naval Architecture
And Ocean Engineering

The demand for LNG has been on the rise for the past few years. Hence the concept of very large LNG carriers is being considered by many shipyards today. The designs are however limited by dimensions such as the draft, length and air draught that are available at the loading and discharge ports. Ships of such proportions demand larger power. The new range of vessels will have wider beams and shallower drafts. This causes a rethinking in terms of the aft body design and the wake distribution patterns. This thesis investigates the effect of transom stern immersion and stern profile angle in LNG carriers. The transom stern immersion is determined to minimize stern wave resistance. At the stern bottom profile, sufficient clearance is given between the propeller and the hull to reduce propeller-hull interaction. Ships with transom immersions, generate stern waves which have a significant impact on the total resistance of the ship. The resistance contribution of this component, studied in detail, can be reduced to a certain extent. In this thesis, the hull-form of a 200,000 m^3 LNG carrier is considered. Four stern models are made and tested in the CFD package, ShipFlow. No change was made to the forward hull-form. The effects of each stern on the resistance characteristics were compared. A computer program was also made based on the thin ship theory. A major hull profile parameter effecting the stern wave generation, which is the stern profile angle was varied and its effect on the wave resistance was studied. The bulb stern was also modified to change the inflow pattern into the propeller. These results were validated using a commercial CFD software package. This thesis would serve as a fore runner in the stern design of vessels in this size category. A proper understanding of the effect of stern on total ship resistance can also be studied.

NOMENCLATURE

L_{BP}	-	Length between perpendiculars
B	-	Breadth
T	-	Draft
D	-	Depth
C_B	-	block coefficient
Δ	-	displacement
Fn	-	Froude number
Rn	-	Reynolds number
C_{WP}	-	water plane area coefficient
C_M	-	midship area coefficient
Dwt	-	deadweight
F_{rI}	-	local Froude number based on transom immersion
Dp	-	diameter of properller
r	-	correlation coefficient
Φ	-	total velocity potential function
ϕ	-	perturbation velocity potential function
ζ	-	wave elevation
m	-	source strength
σ	-	source density
I_S, J_S	-	amplitude functions
S_n	-	cross sectional area section n
C_F	-	frictional resistance coefficient
C_W	-	wave resistance coefficient
C_t	-	total resistance coefficient
x,y	-	position on trochoidal flow line
I	-	transom stern immersion
Bm	-	immersed breadth at the stern
r_0	-	wave amplitude/ radius of generating circle
R	-	radius of rolling circle

L_W	-	wave length
y_0	-	depth of flow line from the stern hull bottom
δ	-	boundary layer thickness
R_{WB}	-	stern wave breaking resistance
R_{FW}	-	remaining following wave resistance
Rst	-	total stern wave resistance
Cwb	-	stern wave breaking resistance coefficient
Cfw	-	remaining following wave resistance coefficient
Cst	-	total stern wave resistance coefficient
v	-	velocity of water flow out of boundary layer at stern
ν	-	kinematic viscosity

1. INTRODUCTION

1.1 Motive

Natural gas is taking over as the leading fuel resource in the world. For long distance seaborne transportation of natural gas, LNG is one of the most efficient commercial alternatives. From the chart below, Fig 1.1, one can see the rising trend in LNG trade into the following decade.

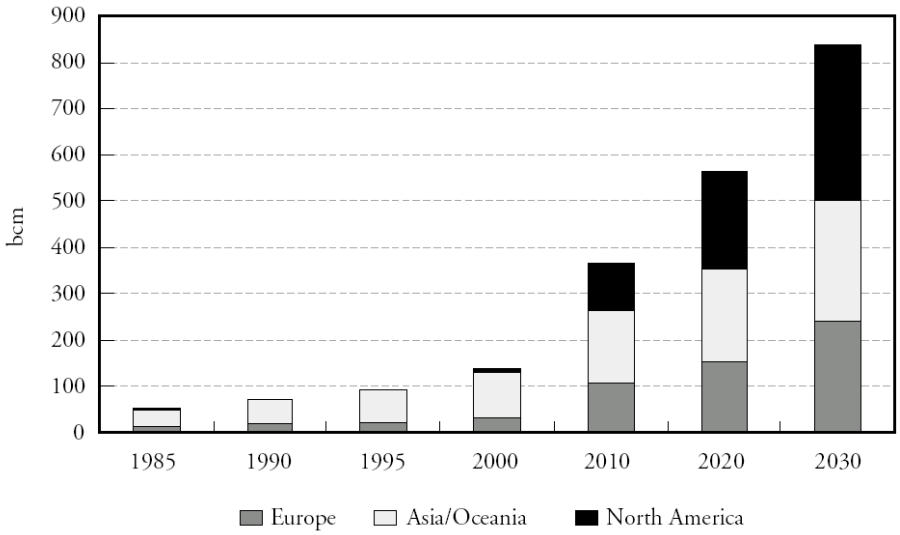

Fig 1.1: Trend of International LNG trade

For this reason the number of LNG carrier orders is increasing. The figure, Fig 1.2 below gives us a better view of the present LNG shipbuilding status.

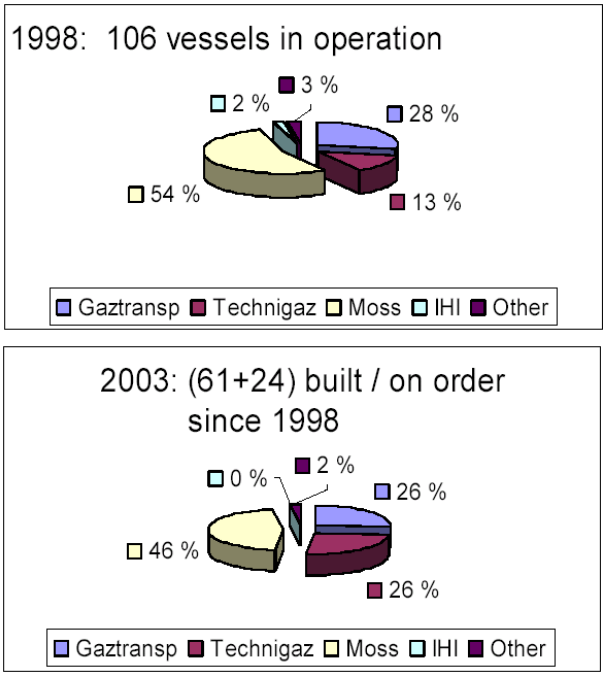

Fig:1.2 LNG ship order break-up (Ref: www.coltoncompany.com)

Oil companies are looking towards larger LNG carriers to cut down on transportation costs. This is leading to a new school of thought in the design of giant LNG carriers. Already, a few major yards have drawn up preliminary designs of LNG vessels in the range of 200,000m^3 to 250,000m^3. The new generation of vessels is expected to have wider hullforms and shallower drafts. So a little rethinking has to be done in terms in terms of the aft body design.

In the race of propulsion alternatives in LNG carriers, dual-fuel engines are the popular choice. But the choice of gas turbine powering is emerging as a contender. When it comes to topside power, the gas turbine is the default choice. The space saving advantage, lesser vibration and maintenance - friendly attributes are its main features. Given below is a

comparison of the engine plant layout showing the possibility of placing the turbine on the poop deck.

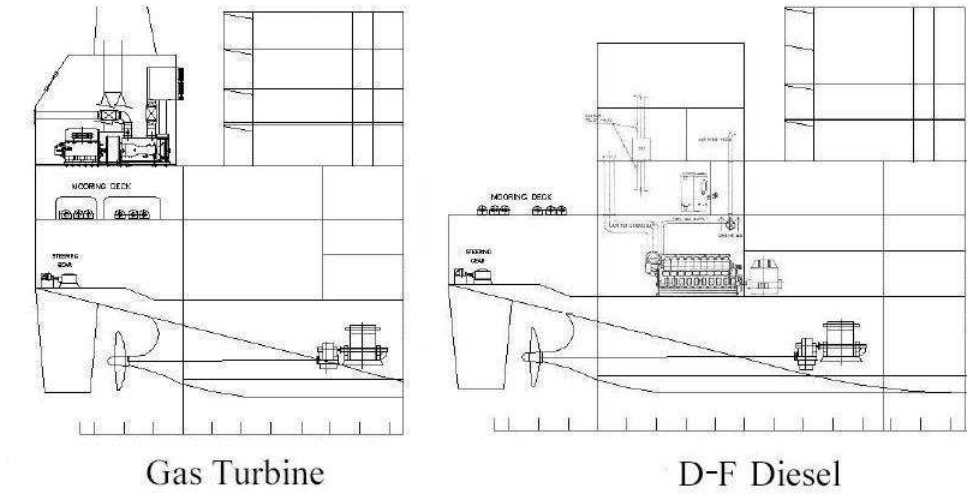

Fig:1.3 LNG ship Engine plant layout comparison [11]

As it can be seen, such an arrangement of placing the turbine on the top can reduce the volume of machinery on the tank top.

The stern design may be quite important for the resistance of a ship and a study like this provides useful information on the desired immersion and the slope of the stern. When a cruiser-stern ship operates at a specific speed or higher, the streamline inside the boundary layer separates. To prevent this, a transom stern is provided. The advantages of this type of stern are:

- due to the shift of the stern pressure disturbance aft of the actual stern, there seems to be a virtual increase in the length
- increase in effective length without weight , wetted area and added frictional drag
- permits easier curvature to the aft hull contour

1.2 Objectives

The analysis of the flow at the stern may be difficult, because of the cavity or “Rooster-tail” collapse that usually occurs at low speeds. In the following paper, the Froude number is considered sufficiently high so that the flow is smooth behind the transom forming a dent on the free surface.

For a ship with transom stern immersion, two stern wave systems are generally created, one from the stern shoulder and the other from the transom. If properly designed, the wave arising from the transom could cancel the stern shoulder waves thereby giving smoother waves and lesser wave resistance.

Here, the stern profile angle is changed and a study is made on its effect on wave making resistance.

2. MAIN DIMENSION FIXING

2.1 Trade Route

In the present paper, the ship is designed to carry LNG from the Ras Laffan terminal in Qatar, to the Incheon receiving terminal in Korea. Fig 2.1 shows the trade route of the vessel.

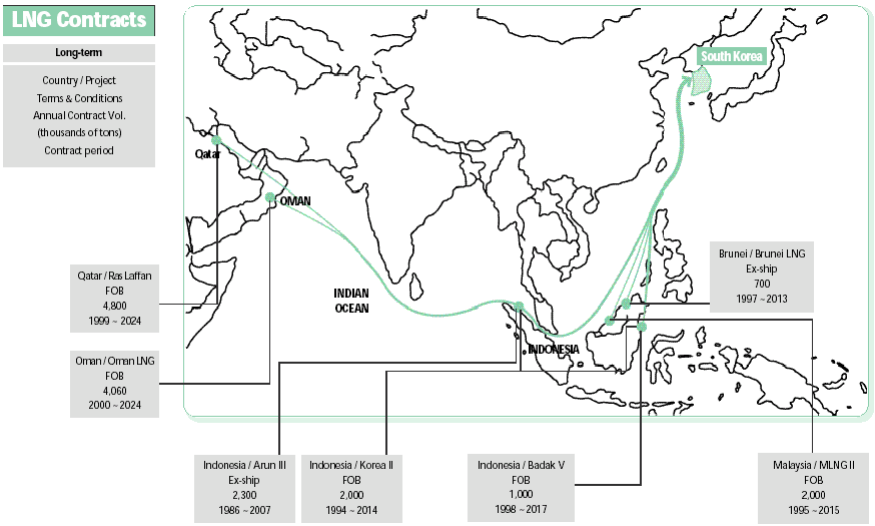

Fig 2.1- LNG trade route

The channel at the Ras Laffan terminal has a maximum and minimum depth of 15 and 13.5 m, and the terminal at Incheon has a depth of 14m. The course is broken in two legs, so that there is a stop at Johore Bahru (Malaysia) port for re-fuelling.

Course details

The ship routes from Ras Laffan into the Indian ocean, passes through the Malacca Straits (minimum channed depth of 23 meters) into the South China seas and in to the

Ras Laffan(Qatar) – Johore Bahru(Malaysia)

Distance – 3604 nautical miles

Duration- 7 days 22 hours @ 19 knots

Johore Bahru(Malaysia) – Incheon(South Korea)

Distance – 2856 nautical miles

Duration – 5 days 16 hours @ 19 knots

The LNG carrier is basically a volume carrier, which means that the main dimensions are fixed based on the required load to be carried. Since the ship under consideration is still in the nascent stage of design, we rely on parametric formulae and parent ship analysis to get a rough estimate of the dimensions.

2.2 Parent Ship Analysis

The main dimension fixing was done by parent ship analysis. The ratios of the main dimensions were calculated. Given below in Table 2.1 is the data assimilated from six different ships. Most of the other ships were parent forms of the ones given below.

Table 2.1- Comparison of selected Parent ship particulars

No	Cargo (m^3)	L_{BP}(m)	B(m)	T(m)	Speed(knots)	Deadweight(t)
1	138000	266	42.6	11.35	20.1	76144
2	138000	266	42	11.3	19.5	76144
3	138000	271	42.5	11.4	19.5	78200
3	145000	274.5	43.4	11.4	19.5	81600
4	147000	270	43.4	11.4	19.5	81600
5	165000	290.5	46	11.5	19.5	82200
6	165000	288.5	48.2	11.8	20.5	83000

From the analysis of the particulars of parent ships, the main dimensional ratios were calculated and are tabulated below:

Table 2.2- Main Dimension Ratio

Ratios	Values(average)
L/B	6.2
B/T	3.81
B/D	1.7
Fn	0.193

The capacity of the vessel is 200,000m3 of LNG. LNG is basically methane which has a density of 425kg/m3. The cargo tanks are only filled up to 98.5% capacity. So the weight of cargo can be estimated to be,

$$\begin{aligned}\Delta c\arg o &= Volume\times\rho\times 98.5\% \\ &= 200{,}000\times 425\times 98.5\% \\ &= 98710.5\,tons\end{aligned} \qquad \text{....(1)}$$

The displacement of the vessel can be estimated by using the cargo deadweight coefficient if the cargo weight is known. The deadweight coefficient is given as the ratio of the cargo weight to the displacement of the vessel. For large tankers the cargo deadweight coefficient is in the range 0.85-0.87. [1]

$$\begin{aligned}\Delta &= c\arg o\, weight / C_{DWT} \\ &= 98710.5/0.85 \\ &= 116130\,tons\end{aligned} \qquad \text{....(2)}$$

2.3 Form coefficients

2.3.1 Block Coefficient [2]

1) Schneekluth

$$C_B = 0.23Fn^{(-2/3)} \frac{L/B + 20}{26} \quad \text{....(3)}$$

The results of optimization calculations provide the basis for the above formula. The above formula is only valid for $0.48 \leq C_B \leq 0.85$ and $0.14 \leq Fn \leq 0.32$.

The range of L/B is 6.18-6.22 for large tankers. For the vessel here, 6.2 is taken. Refer Fig 2.2

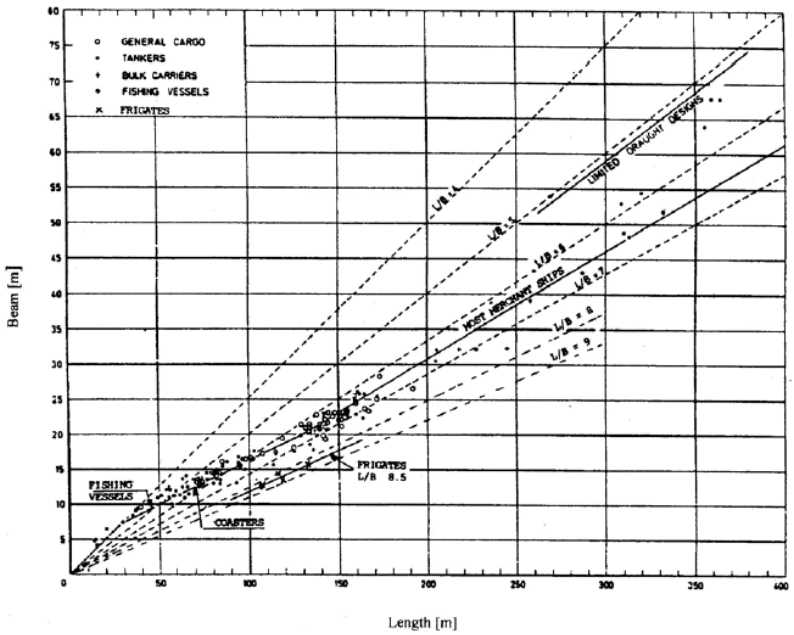

Fig 2.2 – Length vs Beam [8]

2.3.2 Water-plane area coefficient [2]

The water-plane area coefficient influences the resistance and stability considerably. The value of C_W is largely dependent on the sectional shape and CB.

$$C_W = 0.76C_B + 0.273 \quad \text{....(4)}$$

2.3.3 Midship area coefficient [2]

Usually for ships that have a C_M <0.9 a rise of floor is not found. The C_M for such ships is calculated using the formula (6)

$$C_M = 1 - \frac{R^2}{2.33 \times B \times T} \quad \text{....(5)}$$

Where R is the bilge radius

The bilge radius R of both conventional and non-conventional ships without rise of floor can be given by can be given by the formula below

$$R = \frac{BC_K}{\left(\frac{L}{B} + 4\right)C_B{}^2} \quad \text{....(6)}$$

Where C_K =0.5-0.6. A value of 0.5 is taken from parent ship analysis

R is found to be 4.41m

2.4 Linear Dimensions

2.4.1 Length Between perpendiculars

Usually the length of the ship is estimated from similar ships or from formulae and diagrams. The length is a major parameter determining the capital cost and resistance of the vessel.

1) Schneekluth's formula [2]

This formula gives us the length based on optimization results for lowest production costs.

$$Lpp = \Delta^{0.3} \times V^{0.3} \times 3.2 \times \frac{C_B + 0.5}{(0.145/Fn) + 0.5} \quad \text{....(7)}$$
$$= 247.2m$$

Where,

Lpp is the length between perpendiculars [m]

Δ is the displacement [t]

V, speed in knots

Fn, Froude number.

2) Posduinne's formula [2]

This formula is based upon statistics of built ships.

$$Lpp = C\left(\frac{V}{V+2}\right)^2 \nabla^{1/3} \quad \text{....(8)}$$

Where,

The coefficient C is found out by regression analysis of parent vessels and is found to be suitable at 7.4.

V is the trial speed in knots, approximately 1.05 times the service speed = 20.47knots. The range of length is from 245 to 305m.

2.4.2 Breadth

The width is usually fixed as large as the stability demands. The metacentric height is the main criteria for stability. From the parent ship analysis, L/B value was found to lie in the range 6.18 – 6.22. A value of 6.2 was chosen

2.4.3 Draft

The draft is usually restricted by the port and water ways that the ship operates. In the given trade route, the minimum draft is 13.5m. Statistically the draft can be calculated from B/T ratio. This value is taken as 3.83 from parent ship analysis.

2.4.4 Depth

The depth is the cheapest dimension to increase. Also the depth has an advantage of increasing the longitudinal strength. The decision of deciding the depth is guided by the freeboard rules. Here the depth is fixed by taking into account the B/D ratio. For tankers the B/D ranges from 1.6-1.8. In the current problem B/D is taken to be 1.7

2.5 Displacement

The displacement is calculated using the displacement equation

$$\Delta = L \times B \times T \times C_B \times \rho \times (Shell\ correction) \quad \text{....(9)}$$

2.6 Deadweight and cargo weight

The deadweight is the difference of the displacement and the lightship mass. The cargo weight is defined as the difference of the deadweight and the fuel, lube oil, fresh water, crew and effects and provisions. These values are also empirically found out using the formulae in reference [1]

Now by changing the length and keeping the main dimensional ratios a constant, we calculate the various cargo weights. The final main dimensions are selected when the required cargo weight is achieved. Table 1.2 gives the main particular calculations for the different lengths.

Table 2.3 – Particulars at different lengths

L(m)	**245**	**255**	**265**	**275**	**285**	**295**	**305**
B(m)	39.51	41.12	42.74	44.35	45.96	47.58	49.19
D(m)	23.24	24.19	25.14	26.09	27.03	27.98	28.93
T(m)	10.31	10.73	11.15	11.58	12.00	12.42	12.84
Fn	0.204	0.200	0.196	0.193	0.189	0.186	0.183
Cb	0.681	0.691	0.700	0.708	0.717	0.725	0.733
Cwp	0.791	0.798	0.805	0.811	0.818	0.824	0.830
Δ(t)	70246.02	80266.7	91247.51	103239	116292.3	130459.2	145792.2
Steel	17530.83	19575.69	21769.84	24118.09	26625.21	29295.94	32134.99
Outfit	1936.29	2097.58	2265.32	2439.51	2620.16	2807.25	3000.80
E.P.	259.48	323.21	399.21	489.23	595.22	719.29	863.75
L.S.	19726.6	21996.48	24434.38	27046.85	29840.6	32822.49	35999.56
Dwt	50519.42	58270.22	66813.14	76192.15	86451.71	97636.75	109792.6
Cargo	49719.42	57470.22	66013.14	75392.15	85651.71	96836.75	108992.6

From the figure below, Fig 2.2, we can see how the dimensions are selected

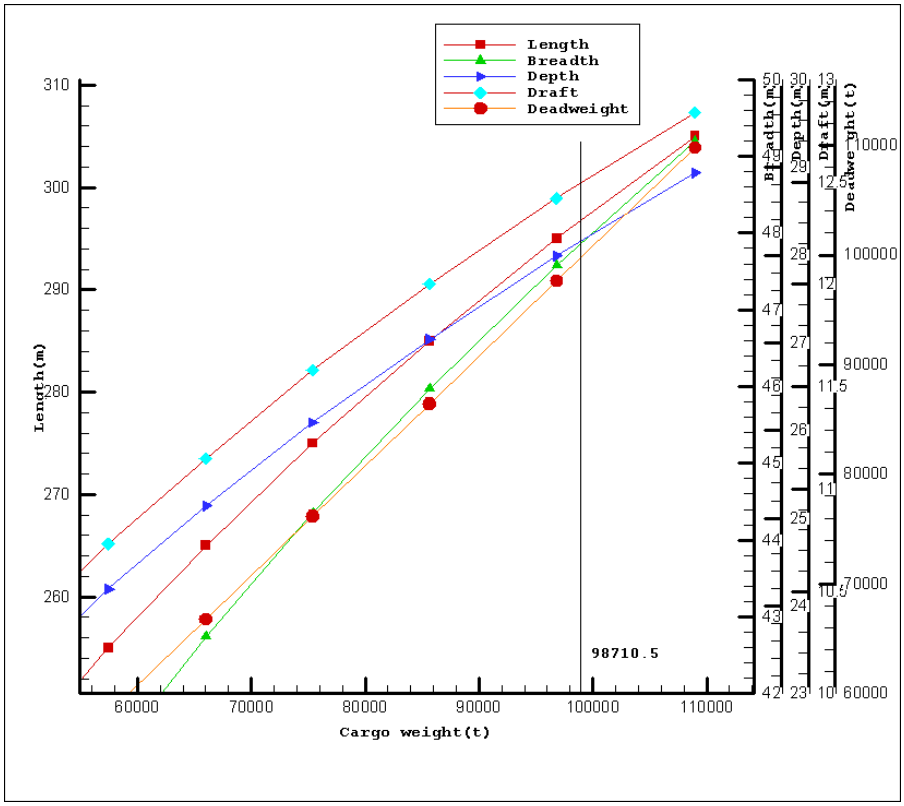

Fig 2.3 – Main Dimension fixing curve

2.7 Volume check [3]

The volume available for the carriage of cargo can be calculated using the formula below:

$$\begin{aligned} Vr &= Vh - Vm \\ &= C_{BD} \times L \times B \times D - Vm \\ C_{BD} &= 0.086\left(D/T - 1\right) + \left(0.7 - C_B\right)0.0475 + C_B \\ &= 0.84 \end{aligned} \qquad \ldots.(10)$$

Where,

Vr is the required volume

Vh is the volume between perpendiculars and below the main deck

Vm is the volume occupied by machinery

CBD is the CB up-to the depth at sides

$$Vm = B(D - D_{DB}) \times L_{ER} \times K \times \left(\frac{K_{ER} aft + K_{ER} fwd}{2} \right)$$

$$K_{ER} aft = {}^{5 \times X_{ER} aft} \Big/ _{L_{BP}} + 0.11$$

$$K_{ER} fwd = {}^{5 \times X_{ER} fwd} \Big/ _{L_{BP}} + 0.11 \qquad \text{....(11)}$$

$$X_{ER} aft = L_{AP} Tank$$

$$X_{ER} fwd = L_{AP} + L_{ER}$$

$$V_{ER} = 52136.15 m^3$$

Where,

LER = 15% LBP = 44.7m

LAP tank= 5%LBP = 14.9m

$\therefore$ Vr = Vh – Vm

= 289753.3m3

The volume is also satisfied.

The results can be summarized as follows:

Table 2.4: Initial Vessel Dimensions

L (m)	298
B (m)	48
T (m)	12.5
D (m)	28.5
C_B	0.73
C_{WL}	0.83
C_M	0.989
Speed	19.5 knots

2.8 General Hydrostatics

On the basis of these dimensions thus obtained, a rough lines was generated using the lines of a 138K m^3 vessel. The hydrostatic details of the vessel were computed using the SIKOB program.

Table 2.5: Important Hydrostatic values

Draft	Displacement	LCB	LCF	VCB	TPC	MCT
10	107998.3	150.198	146.582	5.239	118.648	1922.474
10.5	113942	149.985	145.639	5.501	119.072	1933.518
11	119907.9	149.744	144.72	5.762	119.566	1950.183
11.5	125900.4	149.486	143.914	6.023	120.163	1974.93
12	131926.1	149.214	143.044	6.285	120.963	2012.55
12.5	138000.2	148.919	142.003	6.547	122.007	2065.205
13	144122.7	148.608	141.083	6.811	122.997	2117.342
13.5	150298.6	148.28	140.204	7.075	123.994	2171.137
14	156524.7	147.941	139.378	7.341	124.988	2226.414
14.5	162793	147.6	138.866	7.607	125.717	2265.009
15	169095.9	147.267	138.469	7.873	126.368	2299.208

Draft	GMT	C_B	C_P	C_M	C_{WL}
10	8.89	0.733	0.747	0.982	0.806
10.5	8.296	0.737	0.75	0.983	0.809
11	7.778	0.74	0.753	0.984	0.812
11.5	7.326	0.744	0.755	0.984	0.816
12	6.937	0.747	0.758	0.985	0.822
12.5	6.61	0.75	0.761	0.985	0.829
13	6.32	0.753	0.764	0.986	0.835
13.5	6.069	0.756	0.766	0.987	0.842
14	5.853	0.759	0.769	0.987	0.849
14.5	5.668	0.762	0.772	0.987	0.854
15	5.514	0.765	0.775	0.988	0.858

The final dimensions of the vessel are tabulated below:

Finalized Vessel Dimensions

Table 2.6: Finalized Vessel Dimensions

L (m)	**298**
B (m)	**48**
T (m)	**12.5**
D (m)	**28.5**
C_B	**0.75**
C_{WL}	**0.829**
C_M	**0.985**
Speed	**19.5 knots**

3. HULL FORM DESIGN

3.1 Lines Generation

The lines were developed from a parent vessel. The body plan of the new vessel is as given below:

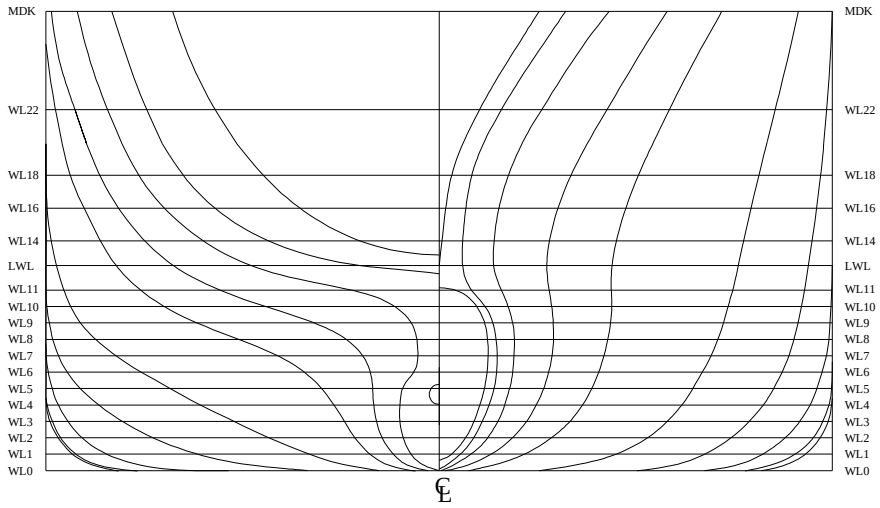

Fig 3.1: Body Plan

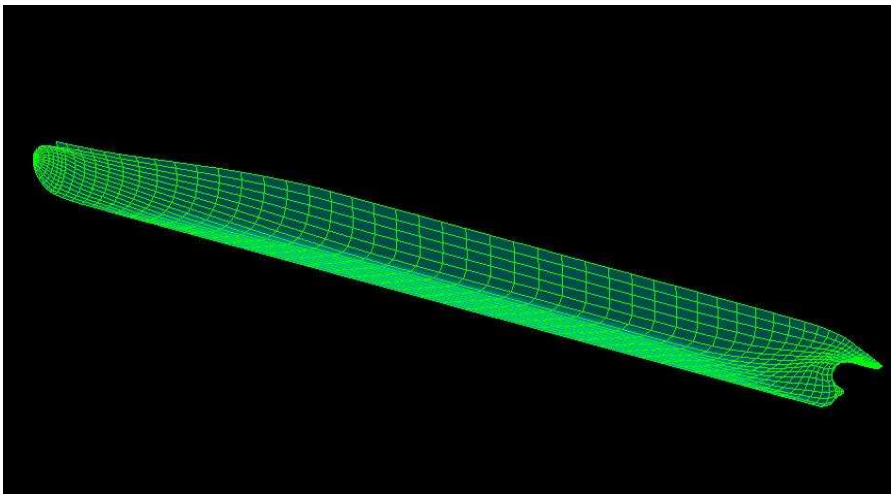

Fig 3.2: Perspective view of ship hull

3.2 Stern Design

Transom sterns are common in modern ships. When immersed the transom stern has many hydrodynamic advantages. The transom stern increases the effective length of the ship, because the stern pressure disturbance appears to be abaft the actual stern. This means that the ship speed could be greater in order to build up a composite stern-wave crest. It also permits considerable easing of the curvatures of the waterlines of the aft body.

The main criteria that govern the stern selection are:

1) Low resistance

2) High Propulsive Efficiency by uniform inflow and better hull efficiency

3) Better vibration qualities

While designing the underwater stern form the following points are to be noted:

1) Reduce flow separation

2) Minimize suction effect of propellers

3) Ample propeller clearance

A bulbous stern is incorporated since it gives the most uniform wake and thus higher propulsive efficiency and less vibration caused by the propeller. The advantages of the bulb stern are offset by an increase in resistance. Depending on the position of the bulb stern, the ship may need more or less power than a ship with a U shaped stern. In the parent vessel an immersed transom is absent. It is intended to introduce transom immersion and also vary the stern profile angles and to study its effect on resistance characteristics. The effects of stern bulb variation will also be studied

3.2.1 Propeller-Hull Clearances [2]

One of the vital points to be noted while designing the stern is the propeller hull clearance. The propeller induced vibrations on the hull is not a function of the propeller diameter but depends primarily on the power and the wake field at the propeller disc. Propeller blades revolving past fixed parts of the ships produce pulses that are transmitted to the hull and to the machinery via the shaft.

The diameter of the propeller is approximated by 2/3T.

Dp = 8.33m

.

Figure3.3 gives a pictorial representation of the clearances

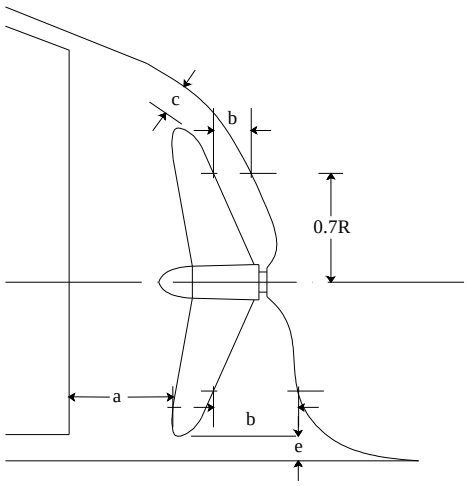

Fig 3.3 : Propeller- Hull clearances

The effects of the propeller clearances can be summarized as follows:

- the vertical clearances c and e should be made as small as possible (optimized not to transmit vibration to the hull) to accommodate propeller diameter
- the clearances a and e should also be small to regain the rotational energy at the rudder section
- b should be large so that the suction decreases more than the wake at that point, thereby improving the hull efficiency.

The clearances are given by recommendations as per rules laid down by the classification society

a> 0.1Dp	= 0.83m
b> (0.35-0.02Z)Dp	= 2.41m (for three bladed propellers)
c> (0.24-0.01Z)Dp	= 1.75m
e	= 0.1-0.2 m in normal cargo ship without heel

3.2.2 Parameters representing the Transom Stern Form

There are three parameters that can define the transom stern

- mean breadth of the immersed aft end (Bm)
- transom immersion (I)
- bottom profile angle (θe)

The stern wave resistance is proportional to the breadth Bm. The immersion determines the stern wave height and the angle determines the stern wave height and the phase shift of the stern wave. Studies on the relation between the three parameters and the stern wave resistance (Yamano et al) [3] have given the following relation:

- stern wave resistance coefficient is determined by the local Froude number, FrI,

$$Fr_I = V \Big/ \sqrt{gI} \qquad \text{....(12)}$$

Where,

I is the stern immersion

Model tests were also carried out to find out the stern wave resistance due to the change in the transom stern profile angle. From the obtained data, the correlation of the transom stern profile angle on the wave resistance can be calculated.

Given below is the coefficient of residuary resistance data on models run at two different local Froude numbers

Table 3.1 Coefficient of residuary resistance Vs. transom stern angle

Local Fn	Angle	δC_r
3.677	0	0
	2.5	0.02
	5	0.045
	7.5	0.1
	10	0.17
3.107	0	0
	2.5	0.03
	5	0.05
	7.5	0.12
	10	0.17

The coefficient of residuary resistance was defined as

$$\delta Cr = Cr - (Cr)_{\theta e=0} \qquad \text{....(13)}$$

This can be considered equal to the stern wave coefficient difference because the same forebody form is adopted for the four models. The correlation factor of the transom stern profile angle on the stern wave was calculated.

$$r = \frac{\sum_{i=1}^{n}(x_i - \bar{x})(y_i - \bar{y})}{\sqrt{\sum_{i=1}^{n}(x_i - \bar{x})^2 \sum_{i=1}^{n}(y_i - \bar{y})^2}} = 0.97 \qquad \text{....(14)}$$

This value of correlation shows that the stern angle plays an important role in determining stern resistance.

As an outcome of the experiments, he constructed a graph that gave a relation between the optimum stern angle (θe), and the local Froude number. Based on these findings, for a local stern Froude number of 4.5, the optimum angle at the stern was zero.

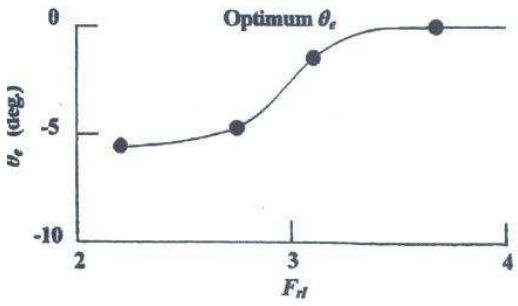

Fig 3.4: Optimum transom profile stern angle [4]

The transom breadth Bm is fixed in order to satisfy the transverse stability. Saunders gives FrI ≥ 4 - 5 as a guide for transom stern design in order fir the transom stern to have

significant wave canceling effects. For the vessel in question, a value of 4.5 is chosen. So the transom immersion was fixed at 0.5m.

Four different sterns are tested. The stern profile is varied by changing the stern profile angle. The first model has no transom immersion, the second has an immersion with a zero stern profile angle, the third has a 5^0 upward angle and in the fourth model, the bulb stern is modified in order to facilitate smoother flow to the propeller disc area. This type of bulbous stern construction has low power requirements.

In Fig 3.5-8, below the four variations of the stern profile are given:

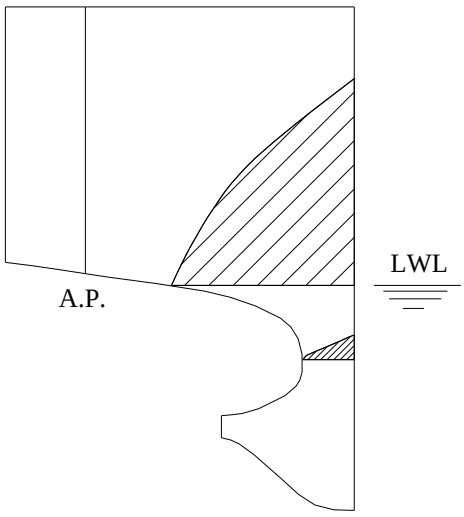

Type 1 - No immersion

Fig 3.5- Type 1 stern

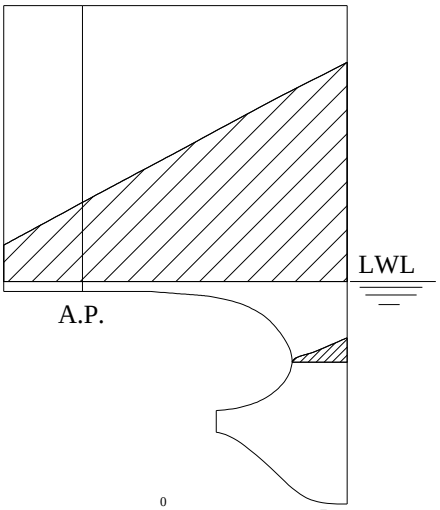

Type 2 - 0^{0} stern angle

Fig 3.6 -Type 2 stern

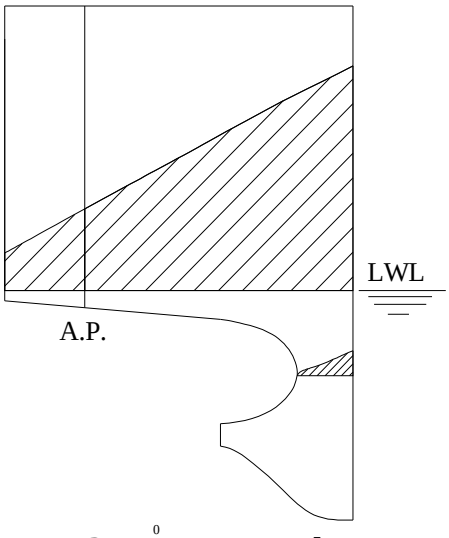

Type 3 - 5^{0} stern angle

Fig 3.7 -Type 3 stern

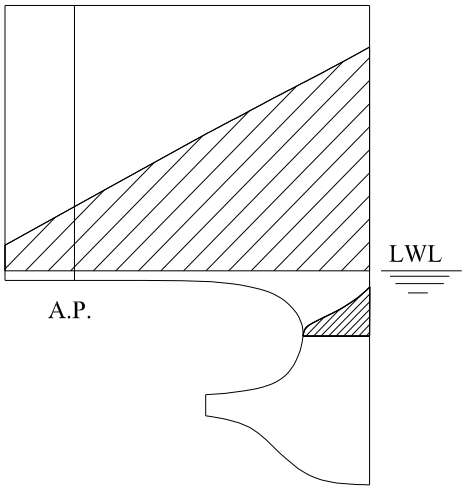

Type 4 - Modified bulb stern

Fig 3.8- Type 4 stern

From the figures above we see that the waterline at the LWL for the Type 1 stern has a sharp curvature while Type 2 and Type 3 sterns have gently sloping waterlines. This helps in minimizing the flow separation. Type 4 stern has a zero stern angle and the deeper curvature before the propeller disc, allowing better flow into the disc.

4. RESISTANCE ANALYSIS OF HULLS

In this thesis a theoretical and computational method will be implemented to calculate the wave making resistance of the various hulls. Havelock's source sink model will be used in conjunction with the thin ship theory for the theoretical analysis and as a simulation tool, SHIPFLOW will be used.

4.1 Theoretical Analysis

The wave-making resistance coefficient was calculated using the thin ship theory applying Havelock's finite source-sink distribution technique. Since the computations are complicated to be done manually, in this thesis, a software package called "Mathematica" was used. The package integrates a numeric and symbolic computation engine, graphics system, programming language, documentation system and advanced connectivity to other applications. This fully "front-ended" application makes it a very user friendly software package.

From Table: 4.1 we can compare the sectional areas of the four different hull forms.

Table 4.1: Section Areas

Station	Type 1	Type 2	Type 3	Type 4
transom	0.00	2.56	1.3	1.3
-0.1	0.00	4.64	2.84	2.32
0	0.00	3.56	9.00	3.6
1	78.00	78.00	78.00	75.28
2	260.00	260.00	260.00	260.00
3	429.18	429.18	429.18	429.18
4	531.45	531.45	531.45	531.45
5	578.76	578.76	578.76	578.76
6	592.27	592.27	592.27	592.27
7	593.81	593.81	593.81	593.81
8	593.81	593.81	593.81	593.81
9	593.81	593.81	593.81	593.81
10	593.81	593.81	593.81	593.81
11	593.81	593.81	593.81	593.81
12	593.81	593.81	593.81	593.81
13	593.61	593.61	593.61	593.61
14	589.57	589.57	589.57	589.57
15	570.00	570.00	570.00	570.00
16	507.32	507.32	507.32	507.32
17	385.85	385.85	385.85	385.85
18	223.98	223.98	223.98	223.98
19	93.55	93.55	93.55	93.55
20	48.85	48.85	48.85	48.85

4.1.1 Linear Thin Ship Theory

The thin ship theory was proposed by Michell in the 19th century. He assumed that the thin ship was lying close to a vertical plane, and so was able to approximate the Neumann boundary condition on hull by a simpler “Michell” boundary condition on that plane. This guaranteed that the ship made only small waves and the nonlinear Stokes conditions on the

unknown free surface could be replaced by a linear Kelvin condition on the known undisturbed free surface. This could be solved analytically by Fourier methods.

Havelock later measured the wave-resistance by calculating the energy in a wave system, made by placing a finite distribution of sources and sinks along the ships centerline. The strengths of the sources and sinks are assumed to be proportional to the slope of the hull surface, the condition being that the total sum of the sources and sinks being zero.

Since the total sum of source and the sink are zero, all the fluid entering at the source will be removed at the sink, so no fluid flows across the body and this space within the confines of the source and the sink can be replaced by a solid body.

Now when these individual sources and sinks are placed in a uniform flow, each of them corresponds to a pressure point moving through the flow. This moving pressure point will give rise to a wave system, and by summing up the individual contributions we can get the wave pattern and calculate the wave resistance of the whole ship.

Before the calculation of the wave resistance, certain assumptions are made:

- fluid is incompressible, homogenous and inviscid
- motion is irrotational and is depicted by a velocity potential ϕ
- wave height is small compared to the wavelength
- any ship shaped forms can be represented by a suitable distribution of sources and sinks

The velocity potential ϕ should satisfy the following boundary conditions

- the normal fluid velocity on the solid is equal to the normal velocity of the solid at every point
- pressure is constant at the free surface of the water
- the velocity diminishes to zero with increasing depth

Co-ordinate system

Here the Cartesian coordinate system is used, where the x-y plane rests on the calm water surface and the positive z axis points upwards. The coordinate system is as given in the Fig:4.3 below

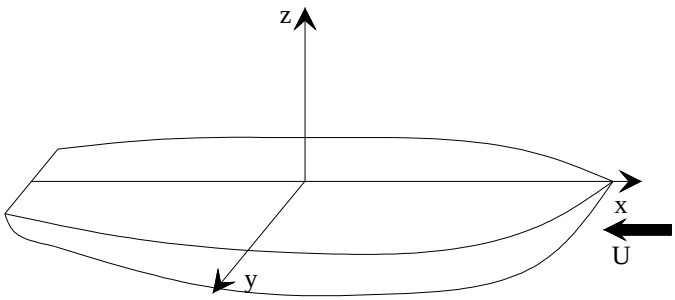

Fig 4.1: Coordinate system

Consider a simple source of strength m, situated at the point (0,0,f).

In order to maintain the second assumption of the velocity potential, we have to add an image source exactly in the mirror image of the first source. This is then superimposed on a uniform flow

$$\Phi = -cx + \phi(x, y.z) \qquad \ldots.(15)$$

Where

Φ is the total velocity potential

ϕ is the perturbation velocity potential due to the ship body

cx is the free stream velocity potential

Applying Bernoulli's equation and neglecting the higher powered terms, we get the wave elevation as,

$$\varsigma = -(c/g)\phi_x \qquad \text{....(16)}$$

From this we can arrive at the free-surface boundary condition

$$\phi_{xx} + K_0\phi_z = 0 \qquad \text{....(17)}$$

Where

$K_0 = g/U^2$

The wave elevation at a very great distance aft can be approximated by

$$\zeta = \frac{4K_0 m}{c}\int_{-\Pi/2}^{\Pi/2} \cos(K_0 x \sec\theta)\cos(K_0 y \sec^2\theta \sin\theta)\exp(-K_0 f \sec^2\theta) \sec^3\theta d\theta \qquad \text{....(18)}$$

Where θ is the angles made by the waves progressing, relative to the direction of motion.

m is the source strength

To make the calculations simpler, the following substitution is done:

$$\sec\theta = \cosh u \qquad \text{....(19)}$$

Wave resistance due to a finite distribution of sources and sinks [4][5]

Ship-shaped bodies with non-mathematical lines can be approximated by a non-continuous but finite distribution of sources and sinks.

The wave resistance can be given by

$$R = 16\pi\rho K_0^2 \int_0^\infty (I_S^2 + J_S^2)\cosh^2 u du \qquad \text{....(20)}$$

Where,

$$I_S = \sum_{s=1}^{n} m_S \cos\left[K_0\left(h_S \cosh u + k_S \sinh u \cosh u\right)\right] \exp\left(-K_0 f_S \cosh^2 u\right) \quad \ldots.(21)$$

$$J_S = \sum_{s=1}^{n} m_S \sin\left[K_0\left(h_S \cosh u + k_S \sinh u \cosh u\right)\right] \exp\left(-K_0 f_S \cosh^2 u\right) \quad \ldots.(22)$$

I_S and J_S are the amplitude functions of the sin and cosine bow free waves respectively.

m_S is the strength of the source

h_S, k_S, f_S are the coordinates of the point source.

Distribution of Sources and Sinks

Consider the normal velocity to the plane y=0 caused by a uniform source distribution over the plane. Let σ be the source density at the point (h,0,-f). Considering an infinitesimally small rectangular surface, δs, around the source, the normal velocity, v, is given by $\pm 2\pi\sigma$. If the surface of the ship is represented by F(x,z), the general boundary condition that the normal velocity of the body and the fluid in contact with it must be the same, can be written as,

$$(c-u)F_x + v - wF_z = 0 \quad \ldots.(23)$$

As per Michell's approximation, the above is simplified and we have the normal velocity as,

$$v = -cF_x \quad \ldots.(24)$$

From this and the earlier definition of v (Eqn 21), we have

$$\sigma = -\frac{c}{2\pi} F_x = -\frac{c}{2\pi} \frac{\partial y}{\partial x} \quad \ldots.(25)$$

The form of the ship is divided into compartments by vertical transverse and longitudinal sections and by horizontal longitudinal sections and the sources in each compartment is replaced by a single source having the same strength as the total strength of the distribution within the compartment and placed at the centroid of the distribution.

Let S1 and S2 be the sectional areas of the longitudinal boundaries of the compartment and V12, be the volume enclosed within it. The total strength of the source distribution is equal to the integration of the source density over the vertical longitudinal section of the compartment.

$$m = \int\int \sigma \, dxdz = -\frac{c}{2\pi}\int\int \frac{\partial y}{\partial x} dxdz \qquad \ldots.(26)$$

This can be written in terms of the sectional areas as,

$$\frac{c}{4\pi}\left(S_2 - S_1\right) \qquad \ldots.(27)$$

From the Fig: 4.2 below we can see how the source strength is represented by the difference in the sectional areas.

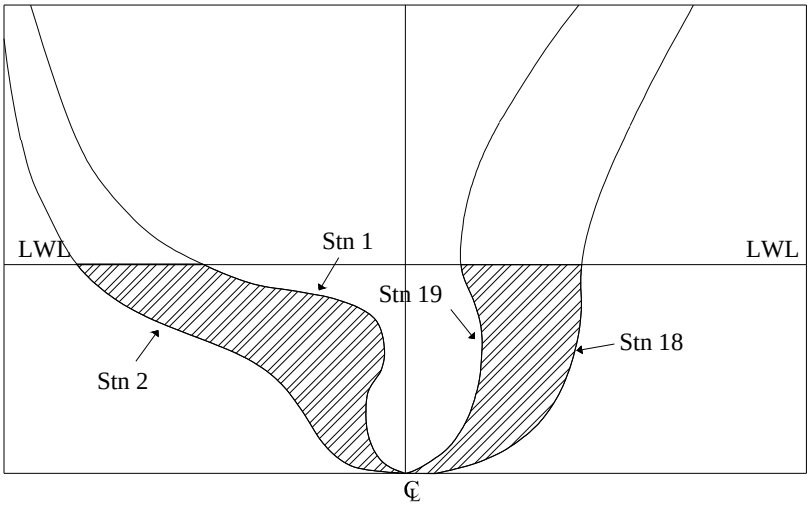

Fig 4.2: Source strength represented by difference in sectional areas

If however, S1>S2, we will have a sink instead of a source.

The longitudinal and vertical position of the centroid of the volume is given by,

$$\bar{h} = \frac{V_{12} - S_1 x_{12}}{S_2 - S_1} \qquad \text{....(28)}$$

and

$$\bar{f} = \frac{V_{12} - S_{1w} z_{12}}{S_{2w} - S_{1w}} \qquad \text{....(29)}$$

Where x_{12} is the distance between sectional areas S_1 and S_2

z_{12} is the distance between the water plane areas S_{2w} and S_{1w}.

4.2 Computational Analysis

The resistance results were computed using the commercial CFD software “SHIPFLOW”. “SHIPFLOW” offers many kinds of subjects corresponding to the “numerical towing tank”, although it is based on some restrictions and simplifying assumptions. This software makes use of three methods to calculate the resistance of the ship- A potential method, a boundary layer method and the RANS equations. Each of these methods is used in the following zones:

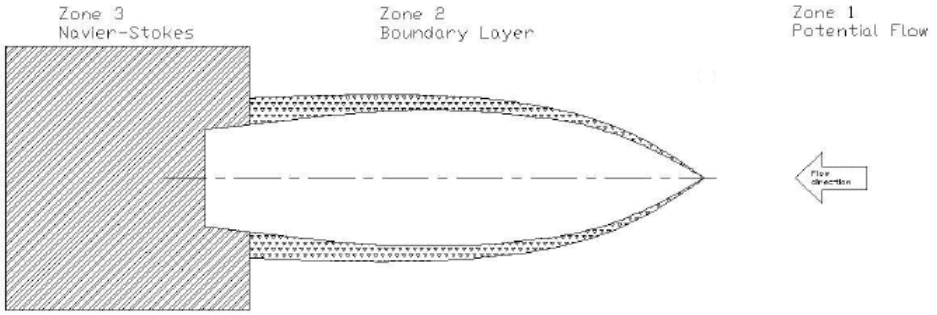

Fig 4.3: Zonal division in ShipFlow

The RANS equations could be used in the whole domain but that would take immense time and memory on the personal computer. The assumption in ShipFlow is that the wave resistance depends on an inviscid process far from the hull and that the viscous resistance is unaffected by the wave making and is occurring close to the hull, in the boundary layer. The wave generation can be modeled by the potential theory and the far field theory. But close to the transom the flow in generally turbulent and therefore the RANS method is used to compute the flow. The shape of the free surface will be compared with the panel code and then the flow under the surface will be computed with RANS, so that all parts of the hull

under the surface will be taken into account after the wave pattern calculation and not only under the still water surface. In ShipFlow, all the data are non-dimensionalized. The length of the Lwl is used for the non- dimensionalization and so the displacement of the vessel will be the one of the real vessel divided by Lwl^3.

ShipFlow divides the ship body and the free surface into grids. The grid definition in ShipFlow is done as described in Figure 4.4

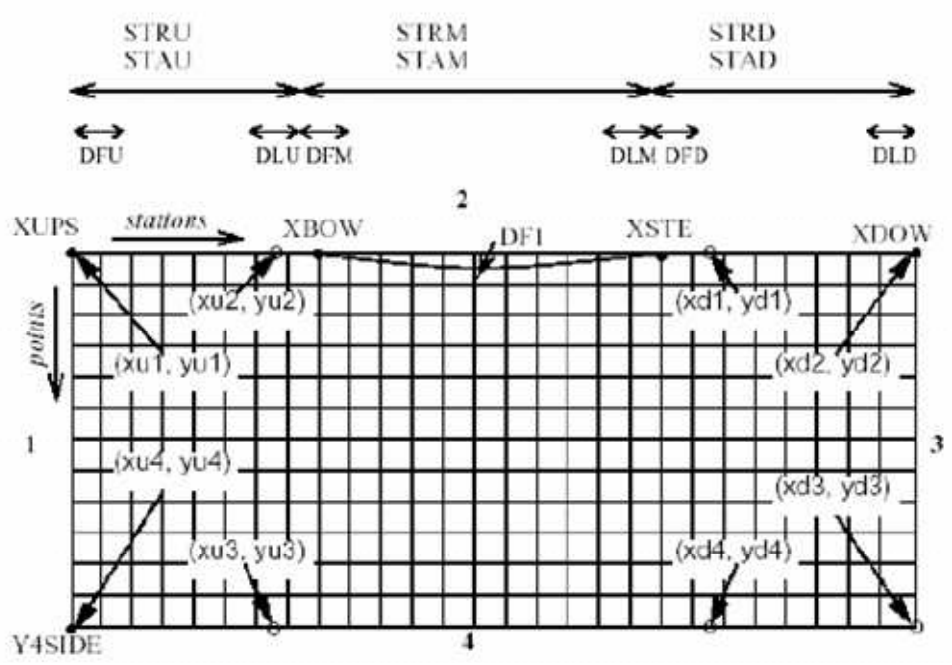

Fig 4.4: Grid Definition is Shipflow [12]

The longitudinal points are called stations and along the beam, points. the ship is placed between XBOW and XSTE. XUPS and XDOW are the extreme ends on the free surface upstream and downstream, respectively. STAU, STAM and STAD are the number of stations in the region between XUPS and the bow, along the ship and between XSTE and XDOW. Since in the present thesis, emphasis is laid on the transom immersion, a transom grid is present to obtain better results.

There is a physical and a numerical model implemented by SHIPFLOW.[6]

SHIPFLOW calculates the wave-making resistance by representing the flow around the ship mathematically as a function of the pressure and the three components of velocity. The program is split into six modules and SHIPFLOW considers one module at a time.

4.2.1 Physical model

1) Governing equation

The flow is assumed steady, incompressible, invisid and irrotational. Assumption of irrotational flow permits assuming the existence of velocity potential such as

$$q = \nabla \phi \qquad \text{....(30)}$$

Where q is the fluid velocity

The Laplace equation represents the equation of state (conservation of mass)

$$\nabla^2 \phi(x, y, z) = 0 \qquad \text{....(31)}$$

2) Boundary Conditions

a) Free Surface Boundary Condidtion:

i) Kinematic Free Surface Boundary condition:

This established the fact that the surface is the boundary between two immiscible fluids, i.e. the particle velocity normal to the free surface must be equal to the normal velocity of the free surface. So if a potential Φ exists, then

$$\phi_x \eta_x + \phi_y \eta_y - \phi_z = 0 \quad , z = \zeta(x, y) \qquad \ldots(32)$$

ii) Dynamic Free Surface Boundary Condition:

The free surface is in constant contact with the atmosphere, and the pressure on the free surface always remains constant. This means that there is interaction between the gravitational forces acting on the fluid and the dynamics of the fluid motion. Here a modified version of the Bernoulli's equation is used, which includes the dynamic pressure and the hydrostatic pressure simultaneously with the acceleration due to gravity g, and the ship speed, U.

$$g\zeta + 1/2(\nabla\phi)^2 = 1/2U^2 \quad , z = \zeta(x, y) \qquad \ldots(33)$$

iii) Combined Free Surface Boundary Condition:

This is got by substituting Eq (29) in Eq (30)

b) Body Boundary Condition: This requires that no fluid penetrates the body.

c) Bottom Boundary Condition: For infinite depth of water, the fluid velocity is zero.

d) Radiation Condition: Upstream disturbance by a moving ship vanishes at infinity.

4.2.2 Numerical Model and Implementation

Implementation: SHIPFLOW uses a boundary integral technique where Rankine sources are distributed on the hull and on a part of the free surface. It offers a nonlinear free surface boundary condition by solving the exact FSBC's satisfied at points on the exact location of the wave free surface. Initially the double model solution is substituted into the undisturbed free surface equation. And the changed wavy free surface is calculated and substituted into

the free surface from the previous step of iteration. This will be continued till the result converges.

Discretization: SHIPFLOW offers first and high order discretizations of the hull and a part of the free surface. The first order method assumes sources of constant strength are distributed on the panels. In the high order method the source strength vary linearly and distributed on biparabolic quadrilateral panels. They can be also distributed on the free surface as well. SHIPFLOW offers a choice on the number of panels on the hull and free surface and the domain of the computational free surface to be discretized.

Solution: The system of equations for the panel source strengths is solved by Gauss elimination or by an iterative technique.

The resistance is basically divided into two components- frictional and wave making. The frictional resistance coefficient is calculated using the ITTC formula [7] given by,

$$C_F = \frac{0.075}{(\log Rn - 2)^2} \quad \text{....(34)}$$

4.3 Stern Wave resistance

4.3.1 Stern flow model

In this paper, in order to calculate the stern wave resistance the following flow model behind the stern is proposed.

The water flow is broken own into two main parts:

1) The flow that breaks which is in immediate contact with the hull, causing the stern wave breaking resistance

2) The part below the former that does not break and forms the remaining following wave resistance.

3) The flow can be approximated by a trochoidal wave.

The wave breaking at the stern can be explained by the fact that, due to immediate contact with the stern, the water flow leaving the stern does not have sufficient energy to climb the following wave crest and maintain the wave profile. Hence a layer of water breaks.

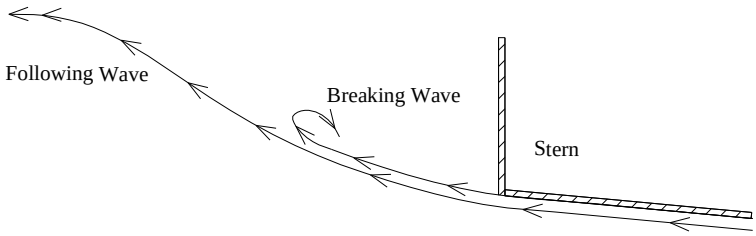

Fig 4.5: Stern Flow model

4.3.2 Approximate water flow behind the stern

The stern wave just behind the transom can be approximated by a two dimensional trochoidal wave. The trochoid is a convenient form, from a geometric point of view. Given below is the representation of the trochoidal wave.

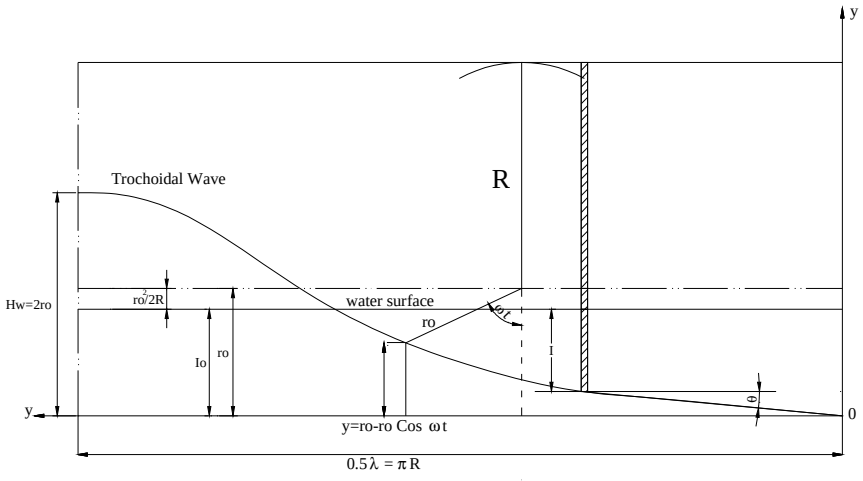

Fig 4.6: Trochoidal wave geometry

Each flow line is represented by the following equations:

$$\begin{aligned} x &= R\omega t + r_0 e^{y0/R} \sin \omega t \\ y &= r_0 e^{y0/R} (1 - \cos \omega t) \\ I &= r_0 \cos \omega t - {r_0^{\,2}}/{2R} \\ r_0 &= \zeta_A \end{aligned} \qquad \text{....(35)}$$

R is obtained from the geometry of the trochoid

$$\begin{aligned} L_W &= 2\pi R \\ L_W &= 2\pi V_S^{\,2} / g \end{aligned} \qquad \text{....(36)}$$

Where Vs is the speed of the ship and L_W is the wave length.

Since the stern angle is quite small the stern angle θ_e can be approximated to zero and the transom stern corresponds to the condition at t=0 and x=0 in this case. Here the stern angle only causes a shift in the phase of the wave as it appends the stern shoulder wave. From Eqn (34), we can find out the value of r_0.

$$r_0 = R - [R(R - 2I)]^{0.5} \quad \text{....(37)}$$

From this equation it can be seen that the wave height is proportional to the immersion at the stern at a constant speed.

4.3.3 Estimation of Resistance due to Wave breaking

The water flow from the hull bottom to $-y_C$ is assumed to break. Usually this thickness lies in the range of 0.19δ (boundary layer thickness). The x component velocity of the water flow after breaking comes to zero near the stern end. Time rate of momentum change of the flow layer due to the x component velocity decrease from u_0 to 0 is therefore considered equal to the wave breaking resistance, R_{WB}

$$\begin{aligned} R_{WB} &= \rho B_m \int_{-y_C}^{0} u_0 dy_0 (u_0 - 0) \\ &= \rho B_m \int_{-y_C}^{0} {u_0}^2 dy_0 \end{aligned} \quad \text{....(38)}$$

Where B_m is the mean breadth of immersed stern

u_0 is the local velocity at a distance y_0 below the hull at the stern.

A local turbulent velocity distribution is assumed at the stern.

$$u_0 / v = (y_0 / \delta)^{1/7} \quad \text{....(39)}$$

$$\delta = 0.37 L_{WL} (\nu / v L_{WL})^{0.2} \quad \text{....(40)}$$

$$v = Vs\sqrt{1 + (2g / Vs^2) I} \quad \text{...(41)}$$

Where δ is the boundary layer thickness

v is the velocity at the water flow out of the boundary layer at the stern

ν is the kinematic viscosity

I is the stern immersion.

4.3.4 Estimation of Following Wave Resistance

Since the wave has been approximated by a trochoid the wave resistance due to the Following waves can be studied by considering the amount of energy in the trochoid wave. The energy in a trochoidal wave can be expressed by

$$dE = \frac{1}{8}\rho L_W \zeta^2(y_0) \quad \text{....(42)}$$

Where, ζ is the wave elevation depending on the depth.

$$r = r_0 e^{y_0/R} \quad \text{....(43)}$$

Where, r_0 is the wave amplitude.

The wave resistance generated at the stern is due to this wave system generated at the and can be given by

$$\begin{aligned} R_{FW}Vs &= \int_{y_C}^{\infty} (dE/T)dy_0 \\ R_{FW} &= (Bm\rho g^{3/2} r_0^{\,2}/VsR^{1/2}) \int_{y_C}^{\infty} e^{2y0/R} dy_0 \end{aligned} \quad \text{....(44)}$$

The total stern wave resistance is the sum of the Wave Breaking resistance and the Following Wave resistance

$$Rst = R_{WB} + R_{FW} \quad \text{....(45)}$$

5. RESISTANCE RESULTS

5.1 SHIPFLOW Results

Stern Type 1

Table 5.1: Shipflow results for Type 1 stern

V_S(knots)	Fn	Rn	Cf($x10^{-3}$)	Cw($x10^{-3}$)
17	0.162	1.995E+09	1.407	0.702
18	0.171	2.112E+09	1.398	0.440
19	0.181	2.229E+09	1.389	0.115
19.5	0.186	2.288E+09	1.385	0.185
20	0.190	2.347E+09	1.381	0.347
21	0.200	2.464E+09	1.373	0.820
22	0.209	2.581E+09	1.365	0.942

V_S(knots)	Ct(10^{-3})	R_T(kN)	P_E	P_B
17	2.118	1395.996	12207.702	19361.939
18	1.846	1364.422	12633.458	20037.205
19	1.513	1245.396	12172.006	19305.322
19.5	1.578	1368.540	13727.552	21772.486
20	1.736	1583.896	16295.118	25844.755
21	2.201	2213.684	23913.098	37927.197
22	2.316	2556.421	28930.507	45885.023

Stern Type 2

Table 5.2: Shipflow results for Type 2 stern

V_S(knots)	Fn	Rn	Cf($x10^{-3}$)	Cw($x10^{-3}$)
17	0.162	1.995E+09	1.407	0.825
18	0.171	2.112E+09	1.398	0.526
19	0.181	2.229E+09	1.389	0.171
19.5	0.186	2.288E+09	1.385	0.138
20	0.190	2.347E+09	1.381	0.347
21	0.200	2.464E+09	1.373	0.729
22	0.209	2.581E+09	1.365	0.993

V_S(knots)	Ct(10^{-3})	R_T(kN)	P_E	P_B
17	2.241	1477.016	12916.206	20485.656
18	1.932	1427.868	13220.917	20968.940
19	1.568	1291.256	12620.220	20016.209
19.5	1.531	1327.780	13318.696	21124.022
20	1.736	1583.622	16292.302	25840.289
21	2.110	2122.157	22924.389	36359.062
22	2.367	2612.641	29566.732	46894.104

Stern Type 3

Table 5.3: Shipflow results for Type 3 stern

V_S(knots)	Fn	Rn	Cf($x10^{-3}$)	Cw($x10^{-3}$)
17	0.162	1.995E+09	1.407	0.822
18	0.171	2.112E+09	1.398	0.526
19	0.181	2.229E+09	1.389	0.160
19.5	0.186	2.288E+09	1.385	0.151
20	0.190	2.347E+09	1.381	0.358
21	0.200	2.464E+09	1.373	0.755
22	0.209	2.581E+09	1.365	1.019

V_S(knots)	Ct(10^{-3})	R_T(kN)	P_E	P_B
17	2.238	1475.038	12898.914	20458.230
18	1.932	1427.676	13219.138	20966.119
19	1.557	1281.944	12529.209	19871.862
19.5	1.544	1338.794	13429.174	21299.245
20	1.747	1593.839	16397.420	26007.011
21	2.136	2147.986	23203.400	36801.587
22	2.392	2640.568	29882.784	47395.375

Stern Type 4

Table 5.4: Shipflow results for Type 4 stern

V_S(knots)	Fn	Rn	Cf($x10^{-3}$)	Cw($x10^{-3}$)
17	0.162	1.995E+09	1.407	0.826
18	0.171	2.112E+09	1.398	0.513
19	0.181	2.229E+09	1.389	0.154
19.5	0.186	2.288E+09	1.385	0.155
20	0.190	2.347E+09	1.381	0.37
21	0.200	2.464E+09	1.373	0.752
22	0.209	2.581E+09	1.365	1.025

V_S(knots)	Ct(10^{-3})	R_T(kN)	P_E	P_B
17	2.24	1477.675	12921.970	20494.798
18	1.919	1418.262	13131.970	20827.867
19	1.551	1277.259	12483.422	19799.241
19.5	1.548	1342.523	13466.580	21358.572
20	1.758	1604.604	16508.170	26182.664
21	2.132	2145.29	23174.282	36755.404
22	2.398	2647.523	29961.484	47520.197

From the comparison curves of the wave resistance coefficients for the three hulls we can clearly see that the Type 2 hullform is a better choice for the service speed.

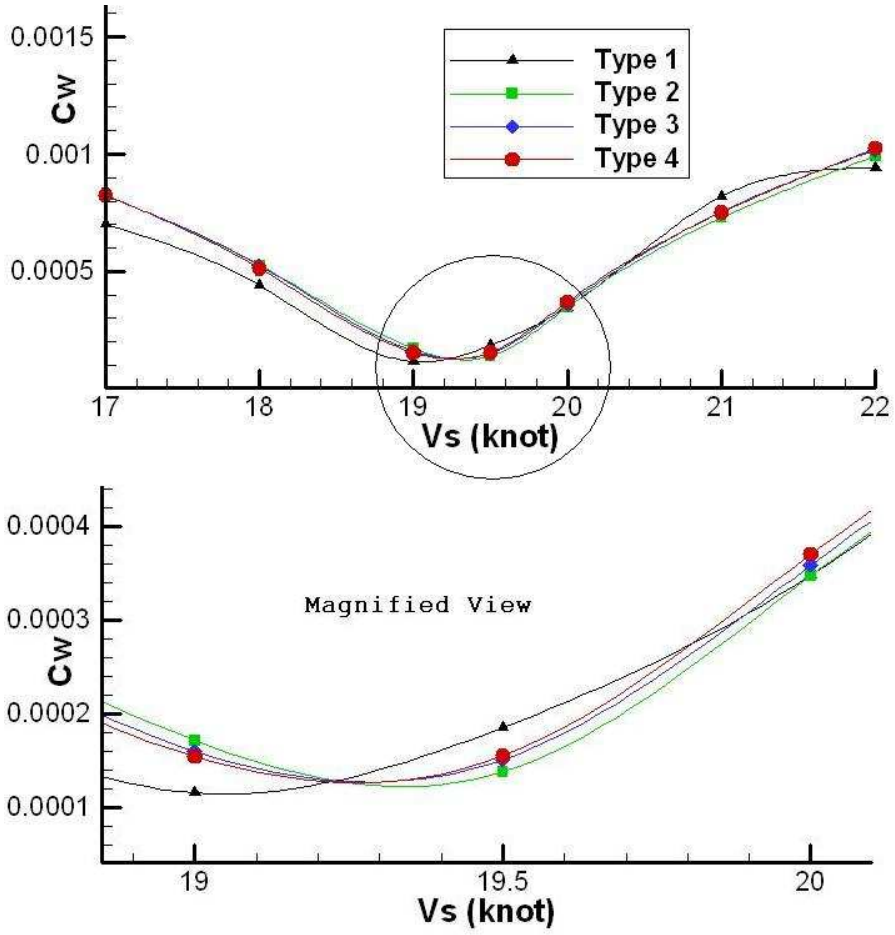

Fig 5.1: Wave-Resistance Coefficient Comparison

Given below is the comparison for the power against velocity curves for the three hull forms

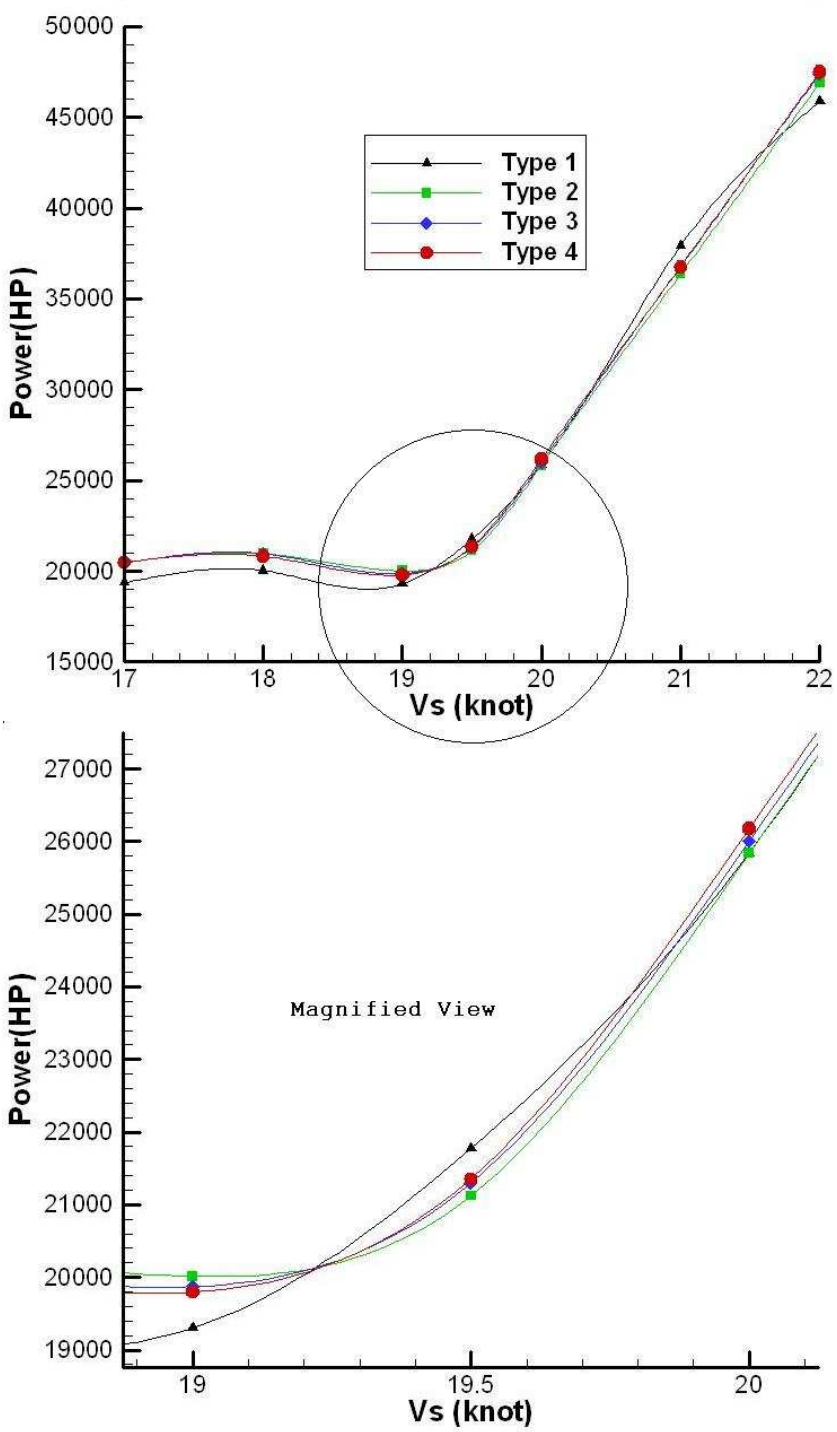

Fig 5.2: Power comparison for the four hull forms

From the resistance analysis it can be found out that the least resistance at the design speed is for a zero degree profile stern form which is in correlation with the test finding of Yamano et.al.

In addition to the resistance, the pressure pattern around the hull and also the wave profile was obtained from SHIPFLOW.

5.1.1 Pressure patterns and Wave profiles

From the figure below, Fig 5.3 ,we can have a comparative study of the Pressure contours and thus see the desired effect.

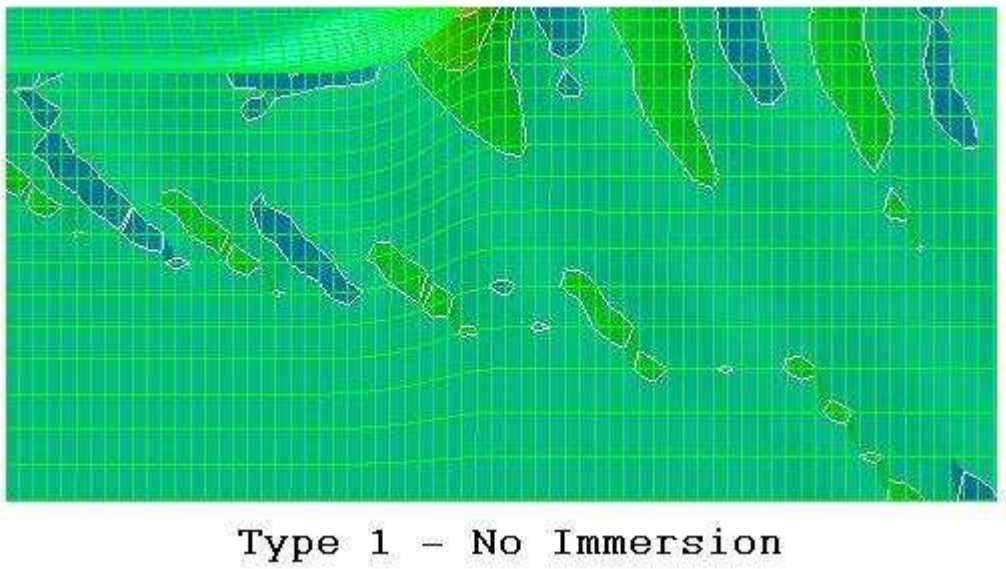

Fig 5.3 – Surface Pressure contours Type 1

Fig 5.4 – Surface Pressure contours Type 2

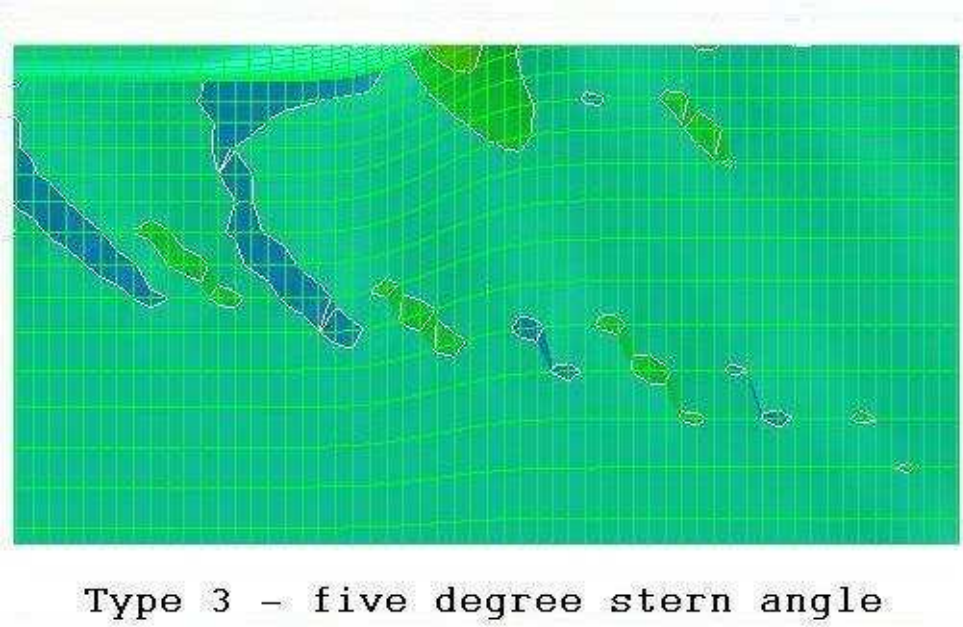

Fig 5.5 – Surface Pressure contours Type 3

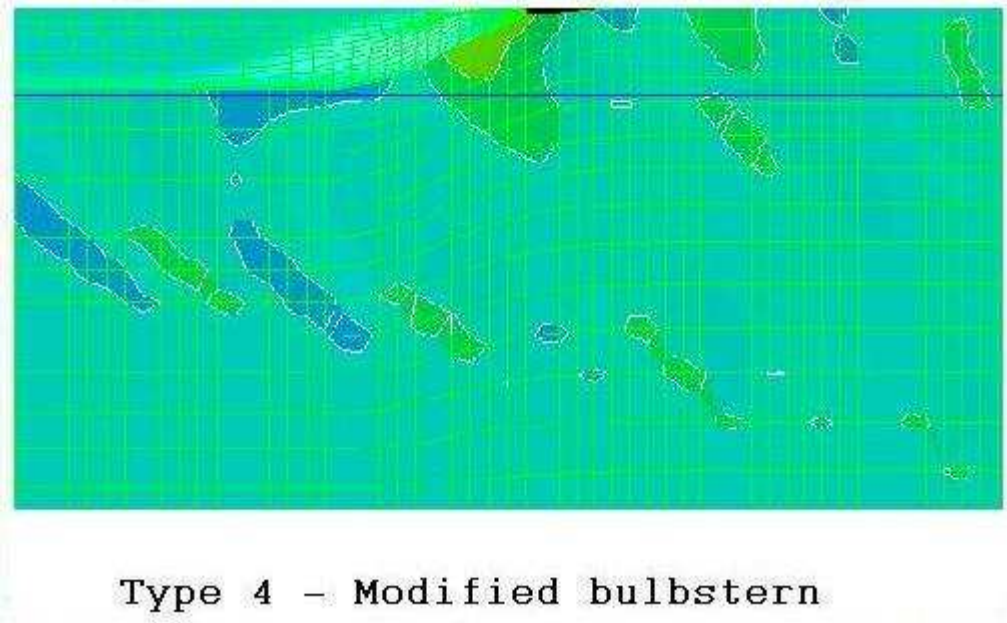

Fig 5.6 – Surface Pressure contours Type 4

Below the comparison of the wave heights due to the introduction of transom immersion, the stern profile angle and the modified stern bulb is given.

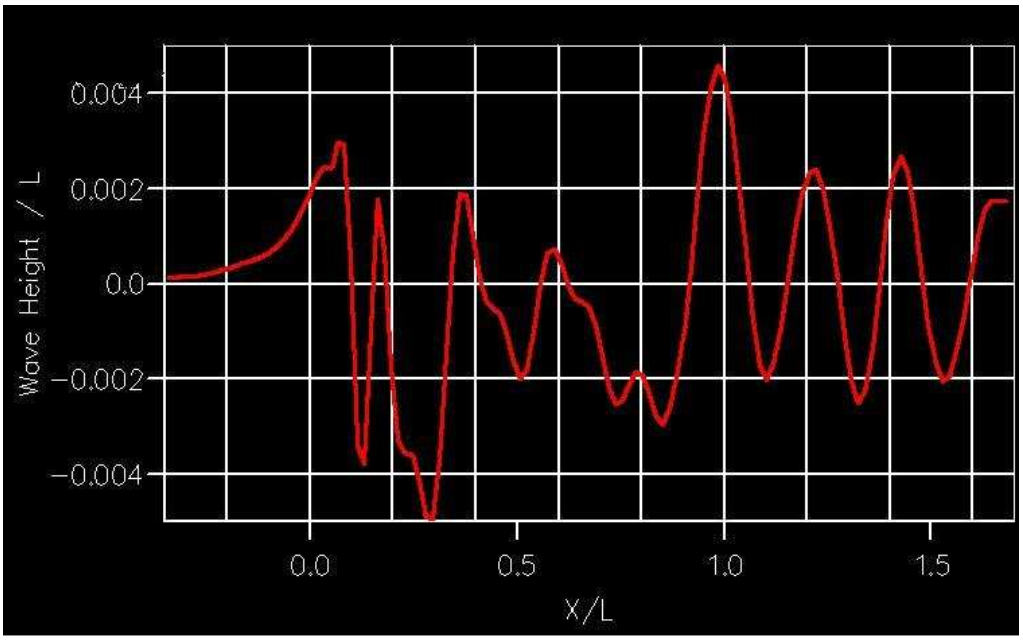

Type 1 – No immerison

Fig 5.7 – Wave-cut Type 1

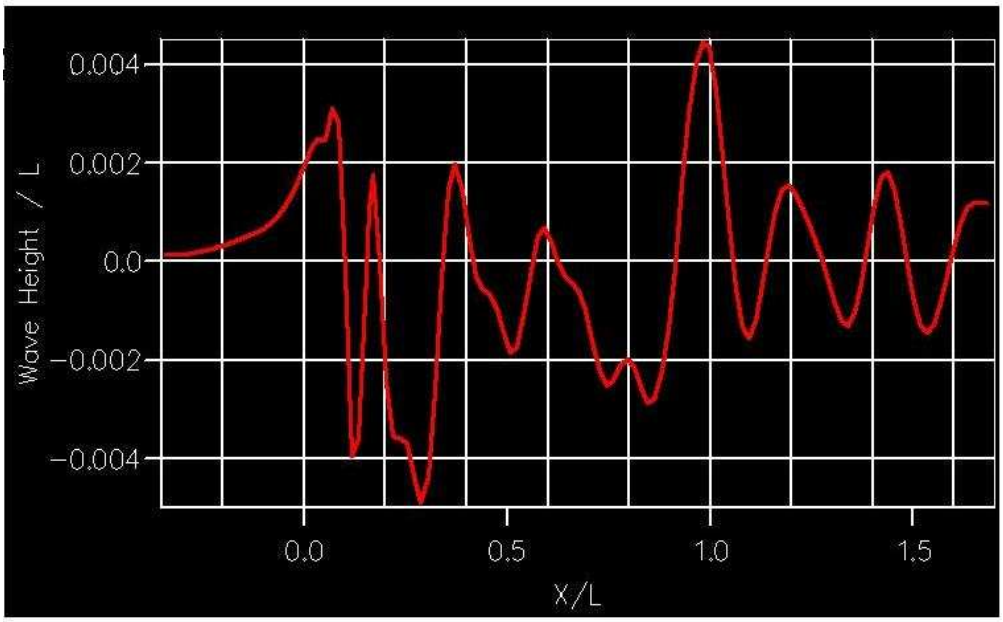

Type 2 – zero degree stern angle

Fig 5.8 – Wave-cut Type 2

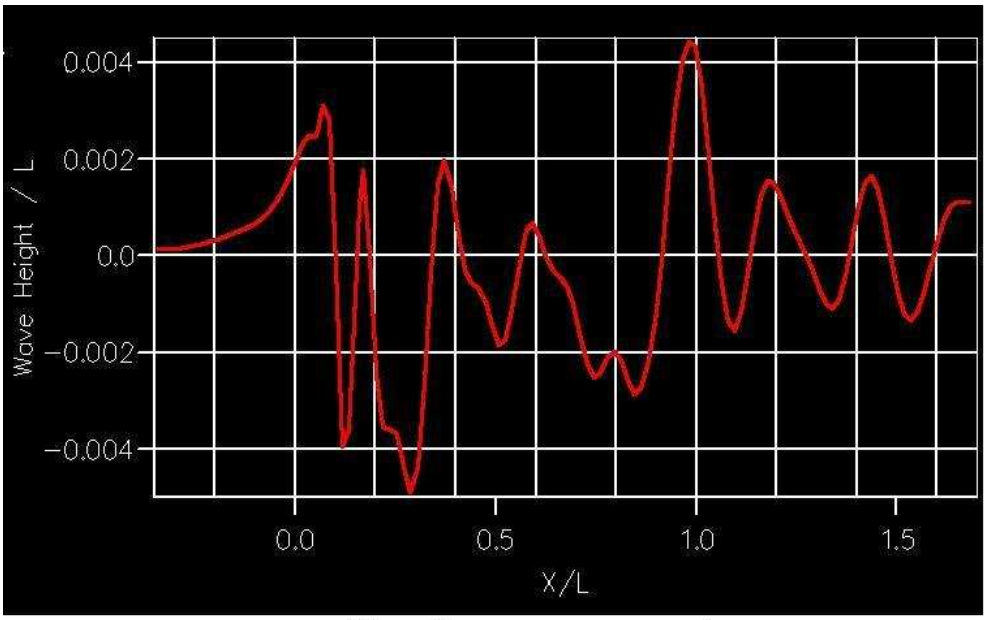

Fig 5.9 – Wave-cut Type 3

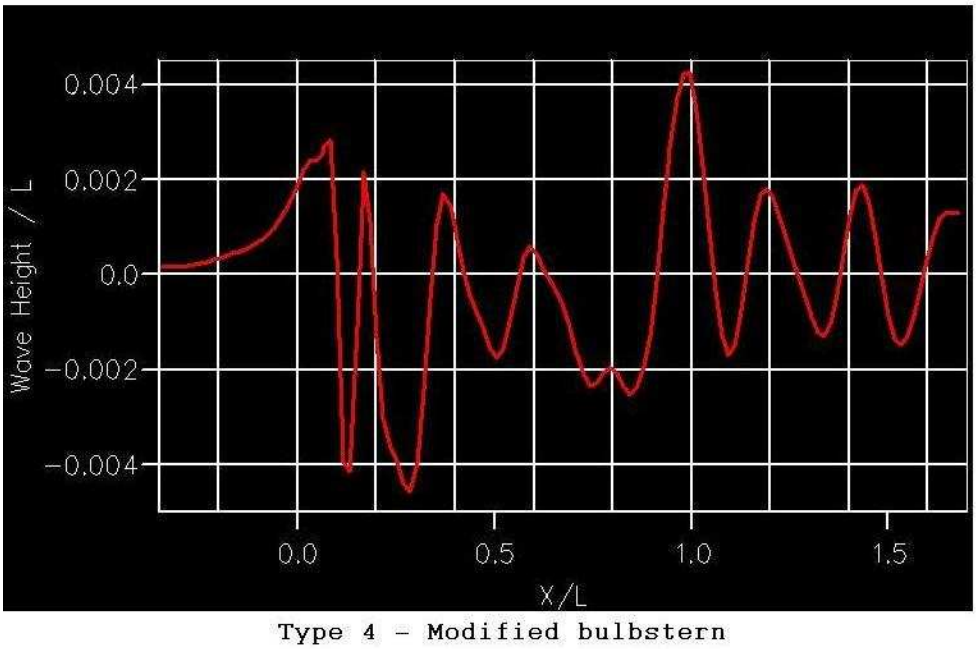

Fig 5.10 – Wave-cut Type 4

Upon close study of the pressure contours and the wave-cut profile it can be seen that the Types 2 and 3 have better pressure contours and wave-cut profiles compared to the Type 1.

Figures 5.5 and 5.6 show a comparison of the flow vector pattern at the stern and the iso wake patterns at the propeller plane between the base hull (Type 1) and the modified bulbstern hull (Type 4) is shown

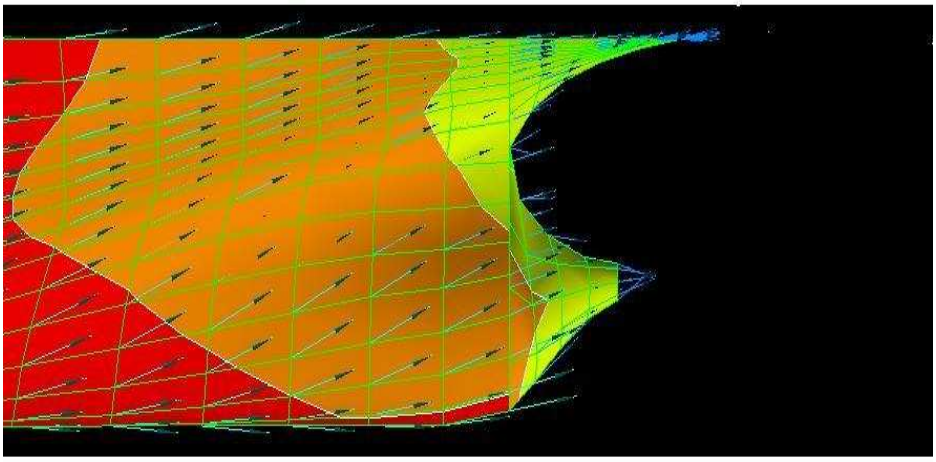

Type 1 – No immersion

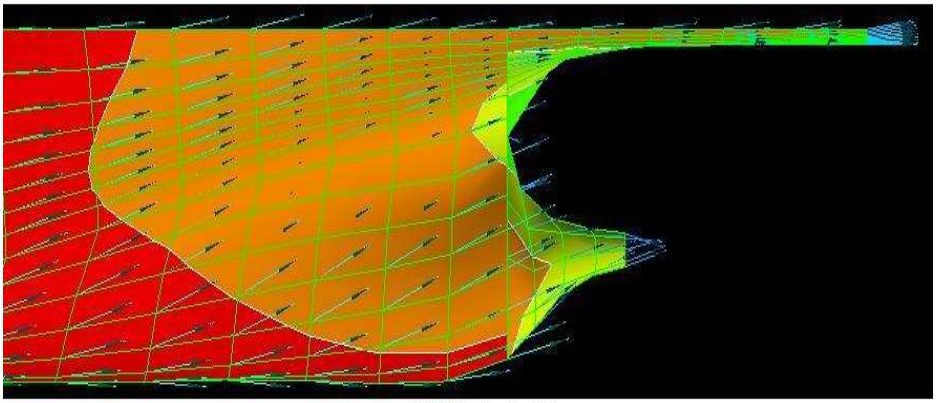

Type 4 – Modified bulbstern

Fig 5.11: Stern flow velocity vectors

This comparison shows how the deeper hull curvature at the propeller disc makes the flow smoother. The tangential flow velocity pattern on the Type 4 hull is better as can be seen.

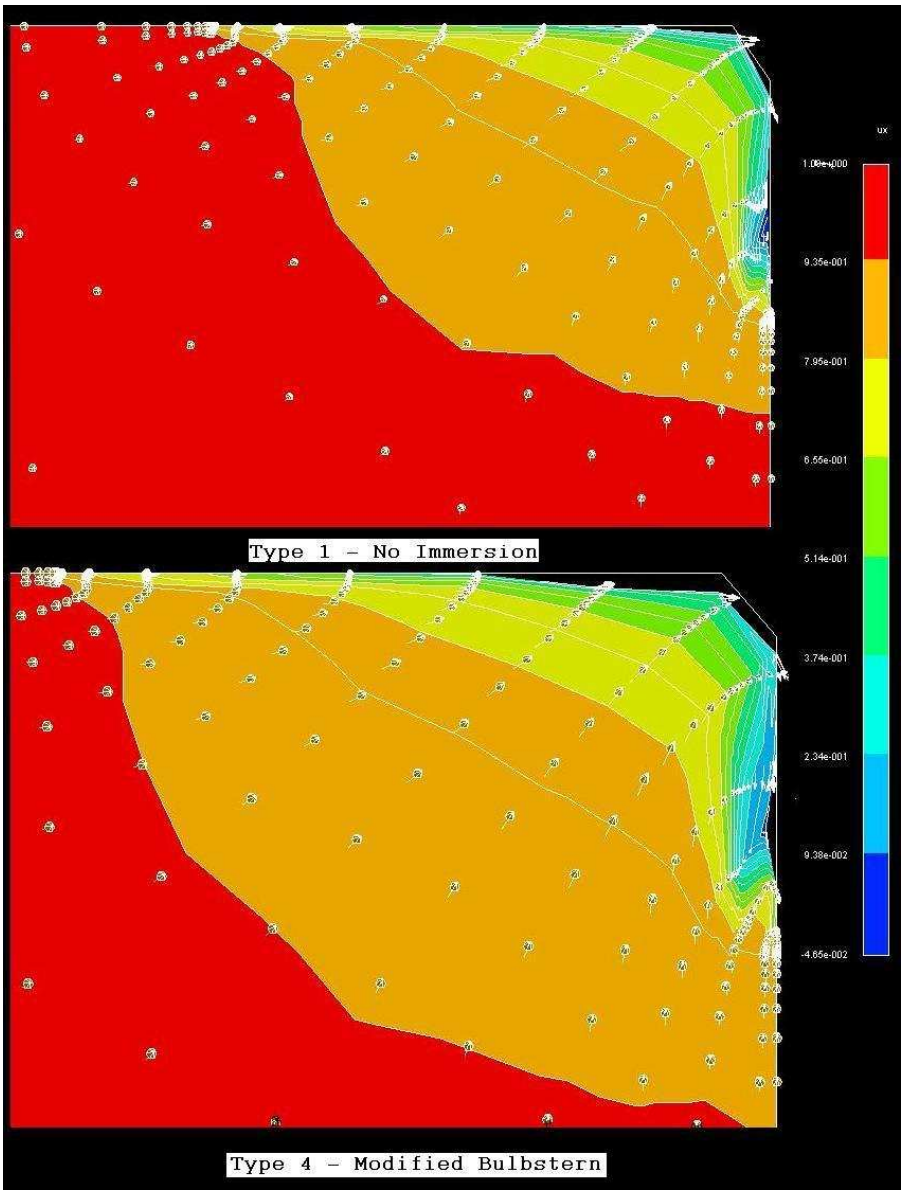

Fig 5.12: Iso Wake pattern

5.2 Thin Ship theory Results

Thin ShipTheory Results Stern type 1

Table 5.5: Thin Ship Theory results for Type 1 stern

V_S(knots)	Fn	Cf	Cw	Rt	P_B
17	0.161736	0.001407	0.000305	1128.94	15658.04
18	0.17125	0.001398	0.000691	1543.58	22668.26
19	0.180764	0.001389	0.000573	1615.37	25040.42
19.5	0.185521	0.001385	0.00097	2041.96	32486.15
20	0.190278	0.001381	0.001418	2552.95	41656.94
21	0.199792	0.001373	0.001183	2570.25	44036.25
22	0.209306	0.001365	0.001253	2890.53	51881.94

Thin ShipTheory Results Stern type 2

Table 5.6: Thin Ship Theory results for Type 2 stern

V_S(knots)	Fn	Cf	Cw	Rt	P_B
17	0.161736	0.001407	0.000185	1049.92	14562
18	0.17125	0.001398	0.000499	1401.96	20588.53
19	0.180764	0.001389	0.000411	1482.36	22978.63
19.5	0.185521	0.001385	0.000777	1874.43	29820.88
20	0.190278	0.001381	0.001182	2337.45	38140.71
21	0.199792	0.001373	0.000973	2359.51	40425.6
22	0.209306	0.001365	0.001071	2689.32	48270.42

Thin ShipTheory Results Stern type 3

Table 5.7: Thin Ship Theory results for Type 3 stern

V_S(knots)	Fn	Cf	Cw	Rt	P_B
17	0.161736	0.001407	0.000228	1066.85	14796.84
18	0.17125	0.001398	0.000573	1413.71	20760.96
19	0.180764	0.001389	0.000475	1493.91	23157.66
19.5	0.185521	0.001385	0.000854	1885.01	29989.11
20	0.190278	0.001381	0.001276	2336.95	38132.55
21	0.199792	0.001373	0.001055	2346.39	40200.83
22	0.209306	0.001365	0.001145	2683.04	48157.69

Thin ShipTheory Results Stern type 4

Table 5.8: Thin Ship Theory results for Type 4 stern

V_S(knots)	Fn	Cf	Cw	Rt	P_B
17	0.161736	0.001407	0.000263	1100.82	15268.01
18	0.17125	0.001398	0.000597	1473.88	21644.65
19	0.180764	0.001389	0.000486	1543.90	23932.56
19.5	0.185521	0.001385	0.000864	1950.05	31023.88
20	0.190278	0.001381	0.001285	2431.59	39676.73
21	0.199792	0.001373	0.001057	2443.59	41866.22
22	0.209306	0.001365	0.001141	2766.93	49663.51

5.3 Stern Wave Resistance Results

The stern resistance is calculated using the method described in Chapter 4. Given below are the results of the stern wave resistance.

The Stern Wave breaking resistance, Following Wave resistance and Total Stern wave resistance are given in Equations (37) and (43) and non dimensionalized by ½ ρ Bm I Vs^2.

Table 5.9: Stern Wave Resistance

Velocity	δ	yc	R	r0	Rwb
17	1.47	0.2793	7.79	0.517	27.48
18	1.45	0.2755	8.73	0.515	30
19	1.44	0.2736	9.73	0.513	32.88
19.5	1.43	0.2717	10.25	0.5128	34.2
20	1.42	0.2698	10.75	0.512	35.55
21	1.41	0.2679	11.89	0.51	39.33
22	1.4	0.266	13	0.509	42.96

Velocity	Cwb	Rfw	Cfw	Rst	Cst
17	0.5394	3.251	0.0638	30.731	0.6032
18	0.5252	3.253	0.0570	33.253	0.5822
19	0.5166	3.251	0.0511	36.131	0.5677
19.5	0.5102	3.259	0.0486	37.459	0.5588
20	0.5041	3.253	0.0461	38.803	0.5503
21	0.5059	3.249	0.0418	42.579	0.5477
22	0.5035	3.244	0.0380	46.204	0.5415

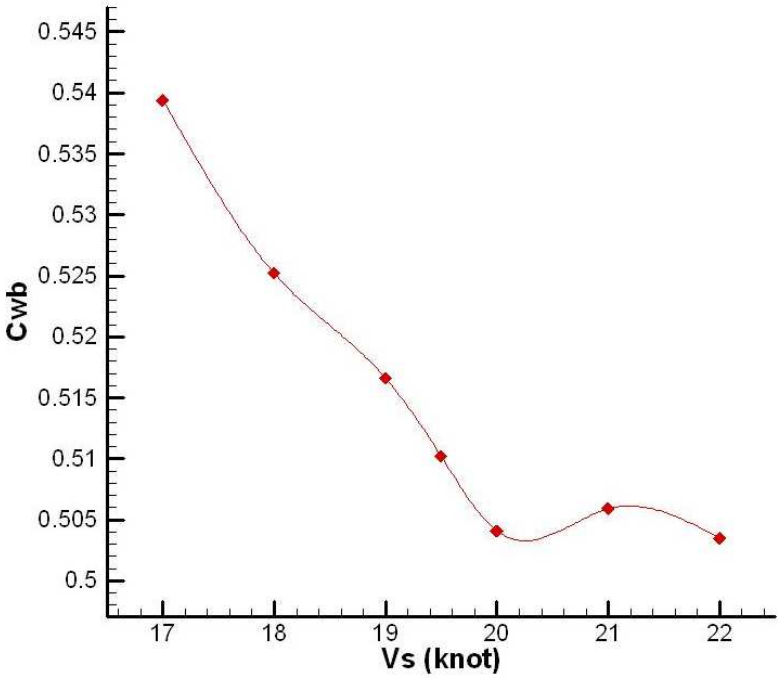

Fig 5.13: Stern wave breaking resistance coefficient

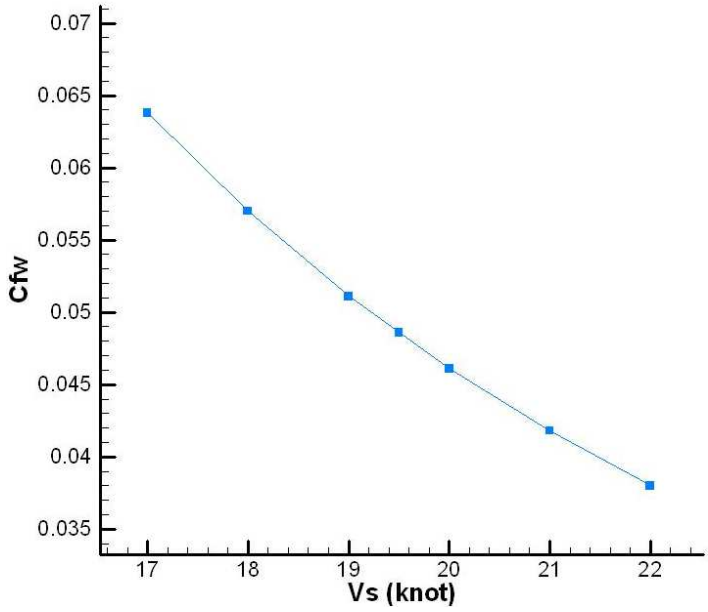

Fig 5.14: Following wave breaking resistance coefficient

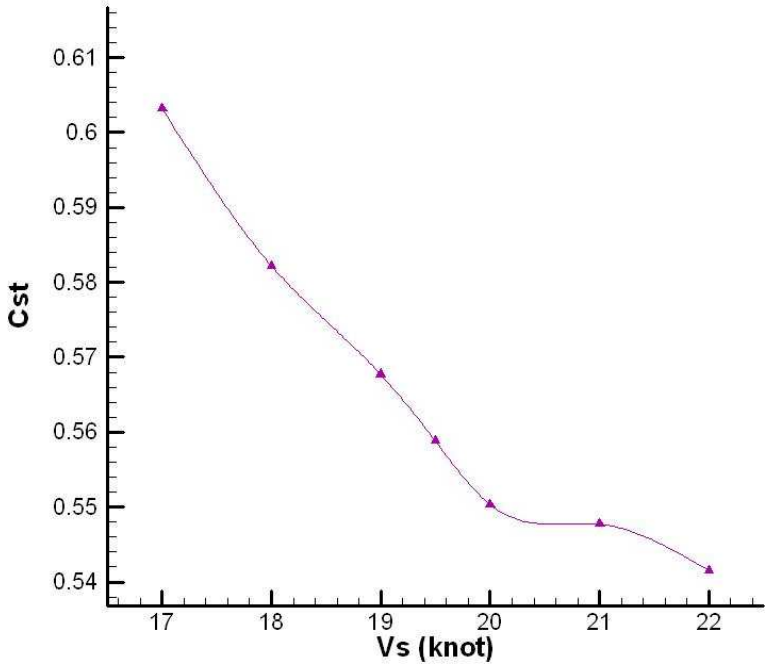

Fig 5.15: Total stern wave resistance coefficient

From the above curves it can be seen that coefficients of stern wave resistance show a reduction as the velocity increases. The stern wave breaking resistance coefficient shows a decreasing trend because it depends on the thickness of the flow layer that breaks. From the resistance data table it can be seen that as the speed increases the thickness of water that breaks, decreases. Hence the stern wave breaking resistance coefficient also decreases. The Following wave resistance coefficient is inversely proportional to the fourth power of the velocity. Hence as the velocity increases, the following wave resistance coefficient decreases as the fourth power of velocity. As a result of the two, the total stern wave resistance also decreases with increasing velocity.

6. COMPARISON OF RESULTS

The wave resistance results obtained from Shipflow and the theoretical analysis show appreciable similarity. Although the results obtained from the theory are not accurate, they can be used to rank the performance of the hullforms. Given below are the comparisons of the results from ShipFlow and the Thin Ship theory.

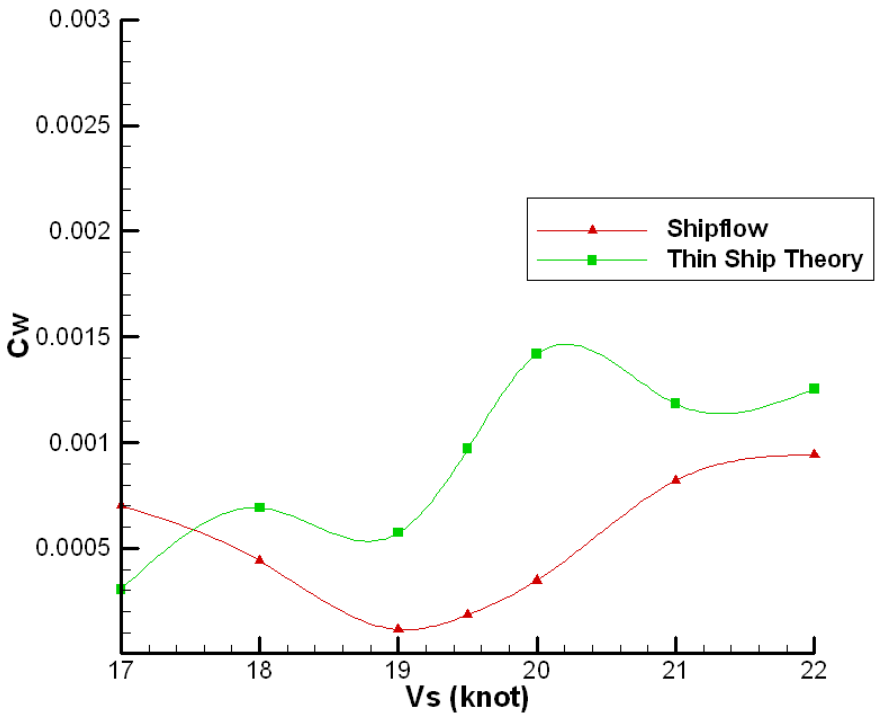

Fig 6.1: C_W comparison for ship Type 1

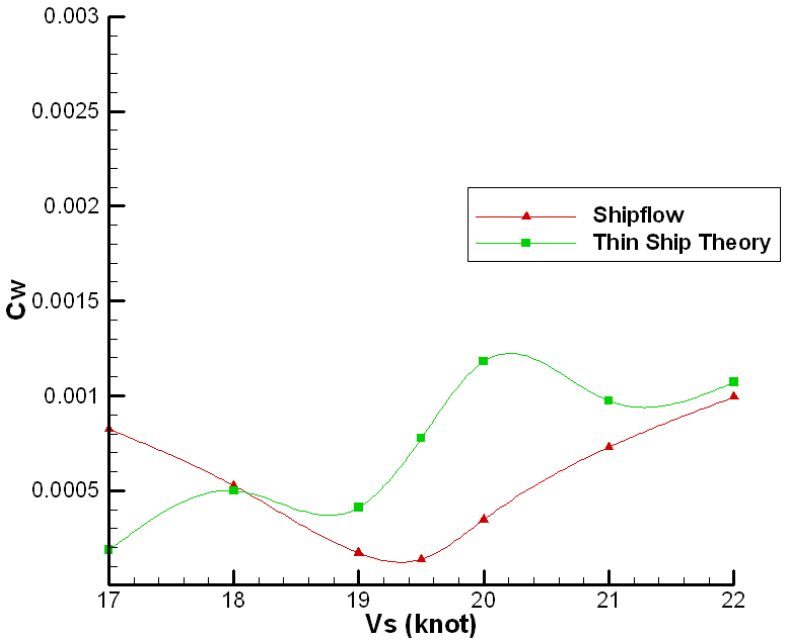

Fig 6.2: C_W comparison for ship Type 2

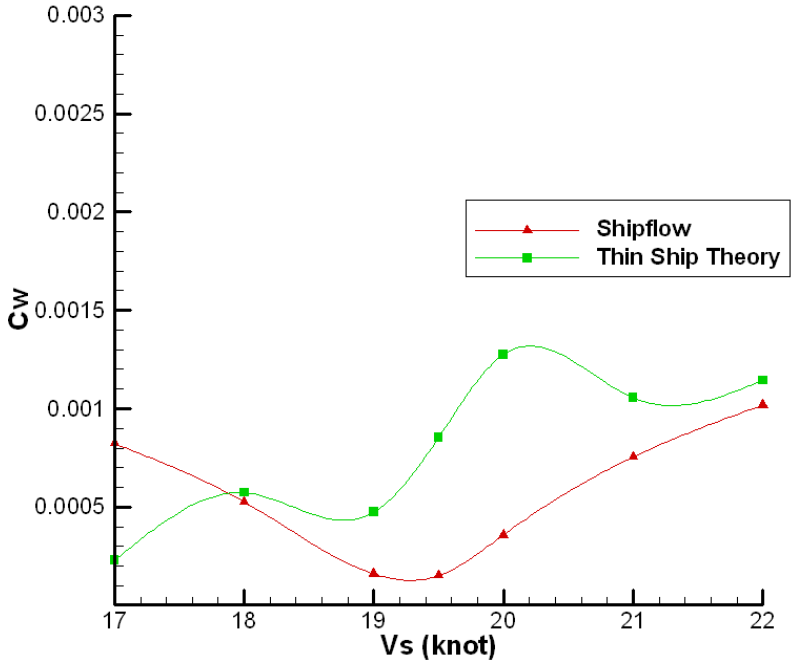

Fig 6.3: C_W comparison for ship Type 3

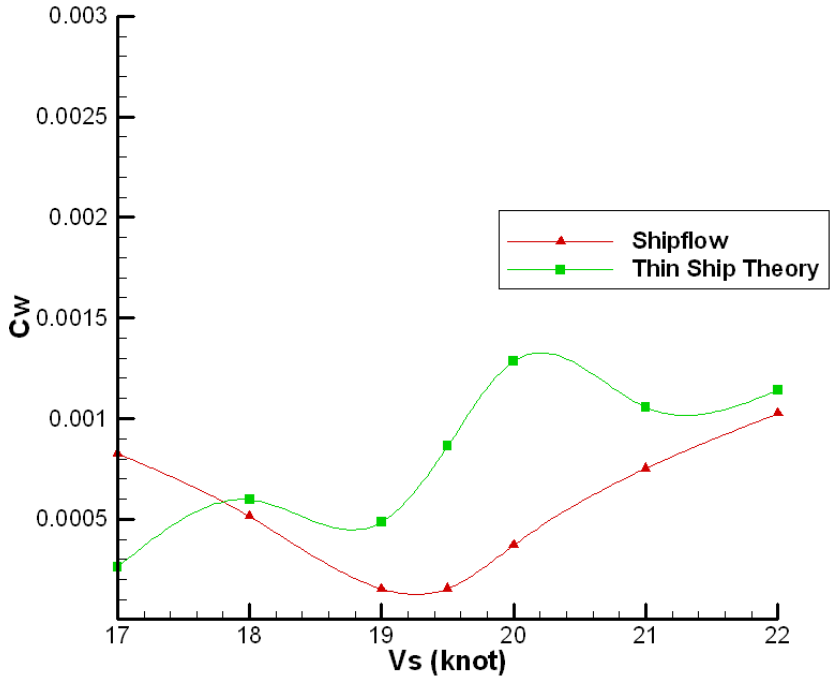

Fig 6.4: C_W comparison for ship Type 4

In the table below, the percentage advantage in the resistance between the Type 1 hull with the Type 2, 3 and 4 are given.

Hull	Rt	δRt	%
Type 1	1368.54	0	0
Type 2	1327.78	40.76	2.97
Type 3	1338.794	29.74	2.24
Type 4	1342.523	26.0	1.94

Table 6.1 – Resistance comparison

Where,

$$\Delta Rt = \left\{ Rt(Type1) - Rt \right\} \Big/ Rt(Type1) \times 100 \qquad \text{.... (46)}$$

Shipflow uses the zonal approach in the analysis of the resistance. Especially in the stern section, where the flow is complicated the Navier – Stokes equation is used. In the theory, a linear model is applied, in order to make the computations easier.

7. CONCLUSION

In this paper, a study was done to find the optimal stern for a 200,000 m^3 LNG carrier. Three stern forms were tested using the commercial CFD package 'SHIPFLOW', and the results were qualitatively verified using the thin ship theory with the application of the finite source sink technique theoretically. The conclusion from this paper can be summarized as follows:

- From both computational and theoretical tests it was found that a zero stern angle yielded around 3% reduction in wave resistance.
- Another observation was that the optimum velocity range for the vessel would be from 18 to 19 knots. The region after that indicates that the ship would be sailing into a hump in the resistance curve.
- The modified bulbstern did not bring about a decrease in wave resistance, but it made a smoother flow into the propeller disc.
- The total stern wave resistance coefficient showed a decreasing trend with velocity for a fixed transom immersion.

REFERENCES

[1] Michael Parsons, “Parametric Ship Design”, University of Michigan.

[2] H. Schneekluth and V. Bertram, “Ship Design for Efficiency and Economy”

[3] H. Schneekluth, “Entwerfen von Schiffen”

[4] Yamano T, Kusunoki Yoshikazu, “A Consideration of Transom Stern Form Design”, Journal of Kansai Society of Naval Architects , Japan, No. 242, Sep 2004

[6] Lunde, J.K., “On the Linearized Theory of Wave Resistance for Displacement Ships in Steady and Accelerated Motion”, Paper presented at the summer meeting of SNAME 1951

[7] Lee, K.J., “Application of Thin Ship Theory to Selection of Least Wave Making Resistance Hullform”, Stevens Institute 1984

[8] Lee Yeon Seung, “Trend Validation of CFD prediction results for Ship Design”, PhD. Thesis Berlin Technical University, May 2003

[9] Lewis E.V., “Principle of Naval Architecture- Second revision, Vol 2”

[10] D.G.M. Watson, “Some Ship Design Methods”, read at the Joint RINA meeting in 1976

[11] D.A. Welch, R.W. Tooke, “Fuelling the future- Powering the Gas Carriers (LNG)”, International Conference - Design and Operation of Gas Carriers, RINA Septmber 2004,London

[12] ShipFlow User Manual, FlowTech International AB